remote sensing

MDPI

Review

From Planetary Science to ISRU: A Review of Remote Sensing and In Situ Measurements for Lunar Resource Prospecting

Simone Pirrotta [1,*], Francesco Latini [1], Abigail Calzada Diaz [2], Giulia Consuma [3], Clive R. Neal [4] and James David Carpenter [3]

[1] Italian Space Agency (ASI), Science and Innovation Directorate, Via del Politecnico snc, 00133 Rome, Italy; francesco.latini@asi.it
[2] European Space Resources Innovation Centre (ESRIC), 28, Av. Des Hauts-Fourneaux, 4362 Esch-Belval Esch-sur-Alzette, Luxembourg; abigail.calzada-diaz@list.lu
[3] European Space Agency (ESA), European Space Research and Technology Centre, Keplerlaan 1, 2201AZ Noordwijk, The Netherlands; giulia.consuma@esa.int (G.C.); james.carpenter@esa.int (J.D.C.)
[4] Department of Civil & Environmental Engineering & Earth Sciences, University of Notre Dame, Notre Dame, IN 46556, USA; clive.r.neal.1@nd.edu
* Correspondence: simone.pirrotta@asi.it

Highlights

What are the main findings?

- A comprehensive review and comparative assessment, revealing the limits of single-instrument resource prospecting.
- An analysis of the emerging lunar ISRU-oriented scenario, offering a forward-looking perspective and strategic recommendations.

What are the implications of the main findings?

- Orientation of the definition of integrated multi-sensor payloads for quantitative resource assessment.
- Promotion of cross-sector synergy to evolve science-driven methods into systematic ISRU prospecting.

Abstract

Lunar exploration is evolving from the traditional science-oriented, government-led sector into a complex ecosystem of disciplines and interests engaging both institutional and private actors. A key factor in this evolving landscape is the necessary sustainability of exploration activities, from the environmental, technical, economic and regulatory viewpoints. This implies the existence of mature technologies for accessing and utilizing local resources, which can support a long-term presence and operations in the lunar environment while potentially fostering the development of a robust space economy. However, it also presupposes the presence of accessible, extractable, and usable resources on the Moon, which remain not yet fully validated. Hence, the first enabling step of this endeavor is a reliable quantitative resource assessment, serving as a prerequisite to orient the critical decisions of stakeholders about strategies and architectures. Available datasets generated primarily for scientific investigation, while foundational, were not designed for these engineering-oriented purposes and currently leave critical gaps in spatial resolution, depth sensitivity, and mineralogical as well as physical characterization. This review examines the status of lunar resource prospecting as obtained by remote sensing and in situ measurement techniques adopted across scientific missions of the last few decades. Existing instruments are systematically evaluated and compared specifically for their capability to

Academic Editor: Jianguo Yan

Received: 8 October 2026
Revised: 13 November 2026
Accepted: 18 November 2026
Published: 25 November 2026

Copyright: © 2026 by the authors. Licensee MDPI, Basel, Switzerland. This article is an open access article distributed under the terms and conditions of the Creative Commons Attribution (CC BY) license.

detect resources such as water and minerals of interest for their use in situ. For each of the analyzed instruments, operational limitations in prospecting for resources independently are identified and assessed, most of which can be effectively overcome through the development of synergistic, multi-sensor instrument suites. Finally, the bidirectional synergy between science and resource utilization, along with future perspectives and strategic pathways for upcoming lunar exploration campaigns, is examined and outlined.

Keywords: sustained lunar exploration; resource assessment; remote sensing techniques; in situ measurements; planetary science heritage

1. Introduction

The Moon has once again become a central pillar of global space ambitions. After decades of limited interest, our natural satellite is today regarded as the next step for humanity's return to deep space, consolidating human presence beyond Low Earth Orbit (LEO) and preparing for the expansion towards other destinations in the Solar System. National space agencies are heavily investing in lunar infrastructure, science, and technology, with goals that go beyond the past United States of America (USA) Apollo program: the Moon is today seen as a nearby and accessible environment to validate technologies and autonomous operations that will be crucial for future exploration missions, notably those targeting Mars. The Moon is also important both as a place of scientific discovery regarding the formation and evolution of Earth's only natural satellite, the Earth–Moon system, and the inner Solar System, and as a platform to explore the universe [1]. Consequently, the Moon has been set as the main target destination in near- and medium-term plans through broad and inclusive programs including "Artemis" as part of the wider "Moon to Mars" architecture [2] (which, during spring 2026, evolved into "Moon Base" [3]) led by the USA, and the "International Lunar Research Station" initiative, led by China with contributions from the Russian Federation [4]. As an expression of the common vision of the member space agencies and governmental organizations, the International Space Exploration Coordination Group (ISECG) has recently released the Global Exploration Roadmap 2024 (GER 2024) [5], which confirms the central role of the Moon as the main target for exploration in this decade. In addition, the Moon retains critical value as a target of scientific investigations, mainly because it preserves key information about the history of the Solar System [6]. Specifically, the study of its quasi-pristine conditions can support the generation of formation and evolution models of the terrestrial planets and their bombardment histories as well as other planetary processes. Without plate tectonics and large-scale mantle recycling, differentiation signatures are better-preserved than on Earth, providing a better record of early planetary processes [7]. Moreover, lunar orbit and surface, due to their unique conditions, can be used to host instrumentation for cutting-edge science such as radioastronomy or imaging interferometry, possibly deployed on the radio-quiet lunar far side [8,9]. Gravitational wave detection could also benefit from sensors deployed on specific lunar regions to obtain high-sensitivity observations in the decihertz band; such an investigation could bridge the observational gap between terrestrial interferometers and future space-borne missions, as proposed in [10].

During the first quarter of this century, this renewed interest in the Moon initiated a proliferation of missions operated by the main spacefaring nations, initially focused on global observation and mapping, and later expanding to in situ measurement and sample return, as recently demonstrated by the Chinese Lunar Exploration Program (CLEP), also known as the Chang'e (CE) Program [11]. Such intense momentum is increasingly supported (mainly in the USA) by the involvement of private companies in what was

previously the exclusive realm of governments, evolving from a purely contractual role into more active and autonomous participation. These actors, promoted in the early stages by institutional programs, notably NASA's Commercial Lunar Payload Services (CLPS), are presently focused on the development of lunar landers as cargo and crew delivery systems, accelerating innovation and reducing the costs of access to the Moon. In the future, their role is expected to extend to other domains for the provision of services within the lunar environment (e.g., communication and navigation or commodities distribution).

This ambitious framework of long-term sustainable lunar exploration can only be made possible by the ability to extract and utilize in situ resources rather than relying on terrestrial supply. The continuous transport of consumables, propellants, and structural materials from Earth not only imposes prohibitive costs but also represents a severe logistical constraint, particularly for missions extending beyond LEO. In contrast, the utilization of local resources has the potential to drastically reduce dependency on Earth-based resupply missions. By enabling the production of life-support consumables, propellants, and construction materials directly at the destination, in situ resource utilization (ISRU) is expected to transform exploration from a series of isolated expeditions into a sustainable and scalable enterprise [12]. Accordingly, ISECG included ISRU among the central elements of the Lunar Surface Scenario elaborated in GER 2024 [5] (Figure 1) and commissioned a group of international experts to prepare a dedicated "In Situ Resource Utilization Gap Assessment Report" [13]. This extensive document examines current capabilities and future needs and improvements, to inform the space community on technology gaps that must be addressed to implement a comprehensive long-term program of human presence in extraterrestrial environments. Beyond its implications for mission sustainability, ISRU is also regarded as a cornerstone of the emerging space economy [14]. Access to extraterrestrial materials could open opportunities for resource-based activities such as lunar and asteroid mining, in situ manufacturing, and the establishment of commercial supply chains beyond Earth. These advancements are not only envisioned as enablers of future exploration architectures but also as drivers of new economic models that could integrate terrestrial and extraterrestrial markets.

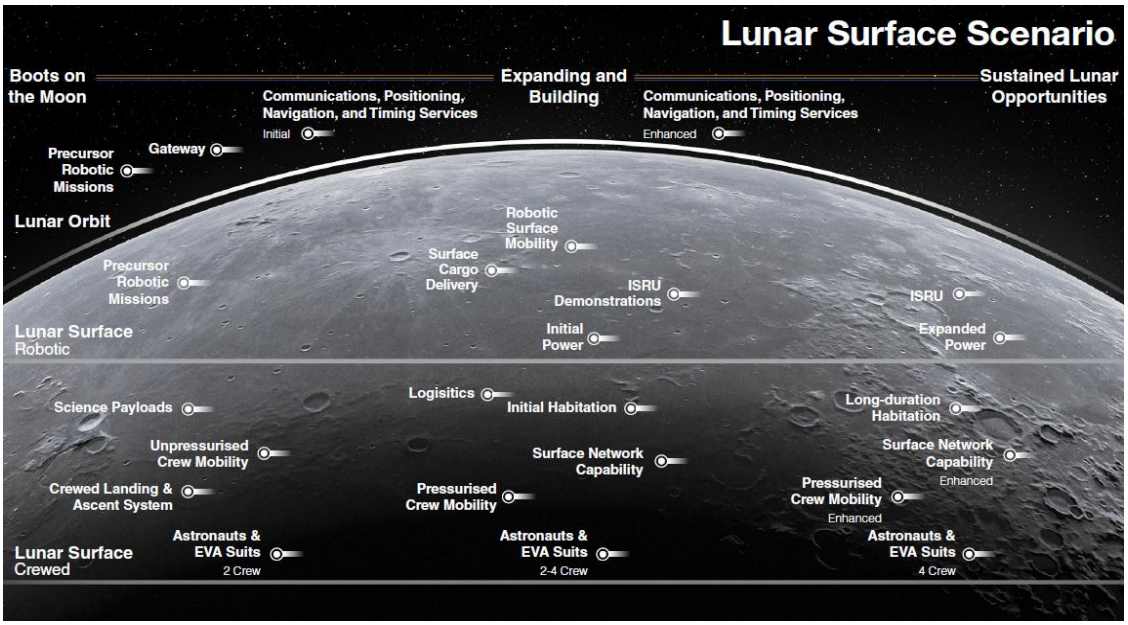

Figure 1. In situ resource utilization among the critical capabilities for the Lunar Surface Scenario, as reported in the ISECG Global Exploration Roadmap 2024 [5].

To avoid ambiguity and ensure clarity, it is useful to specify the terminology adopted in this work. Following the definition established in terrestrial geology by the United States Geological Survey (USGS), a *resource* is defined as "*a concentration of naturally occurring material in such form and amount that economically viable extraction of a commodity is feasible*" [15]. However, in the absence of established markets and operational supply chains, economic viability cannot be demonstrated for any lunar-derived commodity. Consequently, for the time being no economically defined resources can be formally declared under terrestrial classification systems, nor under the Lunar Ore Reserves Standards (LORS) recently proposed [16]. In this work, the term "resource" is therefore used in a prospective sense, referring to concentrations of material that are physically present and relevant for future ISRU applications, rather than those already economically validated. In a broader sense, other elements such as energy extracted from solar radiation, lunar gravitational conditions and its orbital position (e.g., to allow astronomical observations [17]) are also classified as lunar resources, but they fall outside the scope of this paper.

Building on this distinction, two further terms define the stages of resource-oriented investigation. *Resource prospecting* refers to the reconnaissance and screening phase aimed at identifying and spatially constraining materials of prospective interest for ISRU. It typically relies on orbital datasets and limited in situ measurements, is characterized by significant uncertainty and is distinguished from purely scientific exploration by its orientation toward eventual utility rather than pure geological understanding. *Resource assessment*, instead, refers to the subsequent and more structured process of quantitative estimation and characterization of such materials, including the evaluation of their physical properties, distribution, and technical accessibility under defined mission constraints. This stage begins to approach, without yet requiring, the economic criteria embedded in the terrestrial definition of a resource.

For a resource to be evaluated for viable extraction and use, it must first be identified and characterized in both qualitative and quantitative terms. The consolidation of robust methodologies for resource assessment is therefore not only a scientific requirement but also a practical necessity for medium- and long-term exploration initiatives. Resource assessment provides a critical bridge between planetary science, economic feasibility, and commercial viability, highlighting how a deeper understanding of extraterrestrial environments can translate into tangible opportunities for sustainable exploration and space-based markets. While this review focuses primarily on techniques enabling resource prospecting, comprehensive resource assessment is only beginning to emerge through dedicated missions and structured methodologies.

Our knowledge of the Moon's surface and subsurface stems from decades of data collected by scientific instruments onboard orbiters, landers, and rovers, alongside those deployed by Apollo astronauts. Investigations intended to achieve scientific objectives and to answer relevant research questions dictated the requirements, the expected performance and operational profiles for these payloads. This approach, consolidated since the beginning of space science, involved researchers as final users, national space agencies as coordinating customers and industry as implementing contractors.

In this new era of lunar exploration, purely scientific investigation is no longer sufficient or adequate to support the new exploration goals of a permanent human presence on the Moon. The available datasets must therefore be substantially expanded and refined through a campaign of missions designed with specific resource prospecting objectives, advancing from the simple detection of materials to a precise quantification of their concentration and recoverability. Only a credible assessment of lunar resource potential, one that meaningfully constrains abundance, distribution, and recoverability, will allow the engagement of commercial companies as an enabling factor for sustained lunar

exploration. The valuable heritage developed for science-driven missions provides a solid foundation that should now be adopted to mature robust approaches to resource assessment.

This paper summarizes the status of lunar prospecting achieved through remote sensing observations and in situ surface measurements, with a special focus on their relevance for resource identification and characterization. It is organized as follows: Section 2 provides an overview of lunar resource prospecting and identifies the most promising resources for future ISRU. Section 3 describes the main measurement techniques examined and presents a comparative analysis of their strengths and weaknesses in the context of prospecting. Finally, Section 4 discusses the ongoing transition toward dedicated prospecting initiatives and explores their broader implications in a forward-looking perspective, while Section 5 summarizes the main findings of the review and offers recommendations based on the conducted assessment.

2. Lunar Resource Prospecting

2.1. Exploration Science of the Moon

Although sometimes approached independently, planetary science and exploration are deeply interconnected, converging into the discipline of "exploration science". Their synergy has strengthened progressively since the mid-20th century. Initially, the Moon was a remote subject of astronomical and geophysical study, examined via telescopic observations and early fly-by probes. Over subsequent decades, scientific requirements for direct samples, geophysical measurements, and high-resolution surface data transformed the Moon into an active exploration target. The Apollo missions marked the pivotal transition from remote observation to in situ investigation, and the returned samples enabled decisive advances in lunar origin and evolution studies. The systematic investigation of planetary bodies, from remote sensing to in situ measurement and sample return, provides the scientific foundation that justifies and guides mission planning, while exploration missions simultaneously supply the raw observations, samples, and contextual information stimulating new scientific hypotheses in planetary science [7]. A comparative-planetology framework emphasizes how robotic missions reveal the diversity of planetary processes and thus inform our understanding of Earth by analogy [18]. Also, infrastructure and data-handling systems are shown to be critical for turning mission data into robust scientific outcomes [19].

Lunar exploration represents the ideal case study where science and exploration mutually reinforce each other. On the one hand, the Moon holds relevant scientific value, acting as a natural laboratory for investigating fundamental planetary processes across the Solar System [1,20,21]. Numerous orbital and surface missions have targeted the Moon over the past decades to address open questions regarding its origin, accretion, and geological evolution. A comprehensive and systematic synthesis of the primary scientific outcomes from lunar missions operated between the turn of the century and 2020 was recently presented in [22]. Comparing the respective payloads and discoveries achieved, important additional implications were found also in the identification and sometimes quantification of the most critical space resources [23]. What the European Space Agency (ESA) defined as *exploration-focused science* [24] represents problem-driven and mission-relevant research that generates actionable knowledge (such as Space Environment and Effects and Local Resources [25]) required for the effective implementation of successful, safe, and sustainable exploration. On the other hand, lunar surface activities serve as an operational testbed for technologies enabling future deep-space missions; for instance, the lunar surface is being evaluated to depart toward further destinations (though the actual feasibility of this approach is currently under assessment [26]). In this context, *exploration-enabled science* refers to fundamental curiosity-driven or applied research that takes

advantage of exploration infrastructure and data. Ultimately, exploration missions act as both enablers and beneficiaries of planetary science, establishing a virtuous cycle in which science frames exploration and exploration expands science.

2.2. Focus on Resources

One of the most relevant fields of exploration-focused science is resource assessment as an enabler of in situ utilization. A future long-term, affordable presence of human settlements on the lunar surface will be possible only if local resources are used to produce consumables, for life support and exploration needs, including rocket propellants. This will ensure the sustainability of the future human outposts, thereby reducing reliance on periodic resupply missions from Earth [27]. Hence, beyond their intrinsic value in support of scientific investigations, datasets generated from observations of lunar surface and subsurface can inform the space community about the presence, quantity, distribution and accessibility of candidate resources [23]. Scientific results now directly shape exploration architectures. Evidence of polar water, for example, directed the contemporary focus on south-polar landing sites within Artemis and international mission studies. Similarly, recognition of the scientific significance of the South Pole–Aitken (SPA) Basin guides priorities for sample-return missions [28].

Within the framework of exploration, particularly for a primary destination such as the Moon, the materials that have the potential to conveniently generate a commodity are water ice, bulk regolith and the specific mineral phases and elements they contain [29]. As has emerged from decades of lunar study, the lunar surface exhibits a well-established compositional dichotomy: the maria are primarily composed of iron- and magnesium-rich basalts, whereas the highlands consist largely of calcium- and aluminum-rich anorthositic rocks. Confidence in the mineralogical composition of the maria, with abundant ilmenite, pyroxene and olivine, is higher than that for the plagioclase-rich anorthositic highlands, largely thanks to the Apollo returned samples. A comprehensive review of the composition and strategic potential of lunar resources is reported in [30]. The classification of lunar constituents is primarily based on their thermodynamic volatility and mineralogical bonding. It is thus possible to identify two broad categories of lunar resources: volatiles resources (such as water ice, cold-trapped in permanently shadowed regions), and valuable elements chemically bound within refractory lunar minerals and bulk regolith (such as oxygen, iron, silicon, and titanium) [13].

2.2.1. Water and Other Volatiles

The search for water (H_2O) in space was traditionally associated with planetary science and astro-biological goals, whereas today it also represents a key enabling resource for sustainable exploration. Its in situ availability has the largest potential impact on long-term presence, living, and operations far from Earth [31]. Its multiple applications range from supporting Environmental Control and Life Support System (ECLSS) technologies for crewed missions to providing basic elements as consumables for propulsion.

Over the last few decades, scientific payloads onboard lunar orbiters targeted water molecules across different hydration states, as well as their precursor indicators such as hydroxyl (OH) ions. The widespread presence of lunar surface hydration was inferred from the 3 μm absorption feature, which served as a proxy for water and hydroxyl, as globally mapped in [32]. Focusing on permanently shadowed regions (PSRs), the possible presence of stable water ice inside of these cold traps was postulated in [33,34]. The first indications of water at the lunar poles were obtained by the NASA Clementine mission, which initiated the modern phase of lunar remote sensing in 1994, following the early exploration era and the Apollo program. Through its onboard bistatic radar, Clementine measured the polarization of radar echoes versus the bistatic angle β in selected regions.

The measurements observed an enhancement in same-sense circular polarization near zero bistatic angle ($\beta = 0$) in PSRs at the south pole, suggesting the possible presence of water ice in these areas. These observations revealed polarization ratios consistent with coherent backscatter from ice-like materials in permanently shadowed craters near the poles, though rough blocky surfaces can mimic such signatures [35]. To consolidate Clementine's observations, NASA launched Lunar Prospector in 1998, which operated in polar orbit around the Moon for more than one year. While focused on analyzing the Moon's composition and gravity field, it found evidence of abundant hydrogen in the lunar polar regions below at least 40 cm of dry regolith [36]. The orbiter also obtained a global mapping of elemental abundances, revealing strong epithermal-neutron suppression at both poles, interpreted as enhanced hydrogen concentrations suggestive of water or hydroxyl within the upper meter of regolith [37]. Data acquired by Cassini during its fly-by of the Moon in 1999 further indicated the presence of water and hydroxyl on the sunlit lunar surface, with hydroxyl signatures detected especially in the anorthositic highlands at lower latitudes [38].

The first robust detection of hydroxyl and water-bearing species on a global scale was enabled by the orbital spectroscopic observations using the Moon Mineralogy Mapper (M^3) on the first Indian Space Research Organisation (ISRO) lunar orbiter, Chandrayaan-1, which operated during 2008 and 2009. These near-infrared reflectance data enabled the mapping of possible water on the lunar surface and the quantification of OH abundance as a function of latitude, reaching 500 to 750 parts per million. From these observations, it was inferred that surface hydration could result from space weathering and that water molecules may originate from solar wind implantation during agglutinate formation [32]. The Compton–Belkovich Thorium Anomaly on the far side of the Moon was also investigated, revealing the presence of possible water and/or hydroxyl in the region; this hydration was associated with effusive eruptions involving silicic magma, which created a water-rich cap below a magma layer [39]. Another important finding is that surface water abundance varies diurnally, suggesting that the formation and migration of water toward cold traps may be a continuous process. Furthermore, these datasets suggest that water contained in surface pyroclastic materials originates from the lunar interior, consistent with the significant water content predicted in the bulk lunar mantle. Therefore, despite the volatile loss inherent to pyroclastic eruptions, these ancient events effectively transported mantle-derived volatiles toward the lunar surface, turning pyroclastic deposits into potentially accessible reservoirs of volatiles for future ISRU purposes [40].

Important results about the distribution of water on the Moon were obtained by the NASA Lunar CRater Observation and Sensing Satellite (LCROSS) mission, which involved the impact of the upper stage of an Atlas V rocket within Cabeus crater at the south pole, selected because of a large neutron suppression zone identified by NASA's Lunar Reconnaissance Orbiter (LRO) neutron detector [41]. The impact released a plume containing volatiles and water detected through the Near-Infrared (NIR) and Ultraviolet/Visible (UV/Vis) spectrometers onboard a shepherding spacecraft that followed the impactor into the crater. It was estimated that about 155 kg of water vapor were emitted during the impact [42,43].

Recent remote sensing results indicate that hydration signatures are widespread across the lunar surface and vary with latitude, composition, and local time. These hydration signatures water are primarily attributed to structurally bound hydroxyl formed through solar wind interactions, with molecular water also detected, particularly at higher latitudes and colder environments. At lower latitudes, hydration is transient and exhibits a strong diurnal variability [32,44,45]. Nevertheless, the most abundant and potentially usable form of water appears to be the ice trapped in PSRs at the lunar poles [33,36,46]; although its distribution and accessibility are only speculated at the moment [47], its

potential is so critical in driving the interest of the majority of the players towards that region. As elemental components, oxygen (O) is highly abundant in lunar minerals [48], while hydrogen (H) is present in much lower quantity in the regolith and is primarily introduced through solar wind implantation [44], leading to widespread but transient surface hydration [32]. Although mainly endogenous, hydrogen associated with ancient lunar volcanism has been identified in localized materials but its contribution to present surface hydrogen is limited and spatially restricted [49]. Numerous research studies are in progress by research teams to understand and model hydrogen deposition [50], distribution, migration, and combination with and within the lunar regolith [51,52]. Despite the strong interest and exerted effort, the undoubted presence of water on the Moon has not been confirmed yet and it is one of the most urgent questions to be answered in the next few years; definitive feedback will come from dedicated ground-truth measurements [53].

Water belongs to the wider category of *lunar volatiles*, elements or molecules with low boiling points that could easily vaporize due to a temperature change but are temporarily stable under low thermal conditions, usually in permanently shadowed polar craters or embedded in soil grains from solar wind and impacts. In the PSRs, volatiles can derive from cometary and asteroidal impacts or endogenous degassing during early lunar volcanism; outside PSRs, the dominant source is solar wind implantation. In [54], a recent model for the determination of the origin of lunar volatiles is described. Chemical analysis of the LCROSS impact plume further revealed that the most abundant volatile molecules in the impacted area were constituted by water (H_2O) followed by hydrogen sulfide (H_2S), ammonia (NH_3), sulfur dioxide (SO_2), ethylene (C_2H_4), and carbon dioxide (CO_2) [42]. Concurrently, far-ultraviolet observations by the Lyman Alpha Mapping Project (LAMP) spectrograph completed this chemical inventory by detecting carbon monoxide (CO) and molecular hydrogen (H_2), as well as the presence of calcium (Ca), mercury (Hg), and magnesium (Mg) [55]. Beyond their scientific value as indicators of specific lunar geological processes, solar wind volatiles are important for ISRU in the early phase of sustained exploration because they enable the most critical and urgently needed technologies (e.g., propellant production, life support, and chemical synthesis) [56]. Extracting volatiles while preserving their stability will be a key future capability, followed by a dedicated purification step. Indeed, as indicated by LCROSS results, the water ice at the poles is not pure and will need refining before use. Overall, constraining the spatial distribution, abundance, physical state, accessibility, and potential contamination of lunar volatiles represents one of the most critical next steps toward enabling practical ISRU, supporting sustained human exploration, and fostering a vibrant cislunar economy.

2.2.2. Resources in Minerals of Regolith (Key for ISRU)

A solid understanding of elemental distribution and mineralogical characterization is fundamental to the interpretation of the lunar geological history and the modeling of both extinct and active evolutionary processes, improving our understanding of the early Solar System conditions and planetary evolution [57–59]. To this aim, a large variety of scientific instruments have already flown on board orbital and surface platforms and executed a systematic observation and mapping of the Moon. Such a dataset is also directly relevant to lunar resource prospecting and assessment.

The materials currently of highest interest are the oxygen bound within silicates and metal oxides, the KREEP-rich lithologies, the lunar materials rich in potassium (K), the Rare Earth Elements (REEs), and the phosphorus (P), as well as other elements important for science and exploration (e.g., U, Th, and Zr).

The importance of oxygen for exploration is mainly related to its use in support of ECLSS, as well as its role as potential propellant for chemical rockets to be fueled directly on or in orbit around the Moon. It is abundant in the lunar regolith and widely distributed

in most of its minerals, predominantly within silicate minerals (e.g., plagioclase, pyroxene, olivine) and oxide phases such as ilmenite, such that oxygen comprises ~40 wt% of the regolith by mass [30]. Several techniques for oxygen extraction from lunar regolith are currently under study in laboratories, often as adaptation of mining processes for metal reduction, where oxygen is obtained as a secondary product [60]. The most promising technologies under study for optimization include hydrogen reduction of metal oxides, carbothermal reduction [61], and electrochemical methods such as molten regolith electrolysis and molten salt electrolysis [62]. A summary of their thermodynamic fundamentals and current maturity is reported in [60]. Furthermore, solar vacuum pyrolysis represents an alternative option for oxygen extraction, offering the advantages of lower operational temperatures and no need for consumables [63]; it has been recently tested on the EAC-1 lunar regolith simulant, showing a yield of 35 mg of oxygen from a 3.38 g regolith, corresponding to 1.05% of the processed sample, or 2.47% of the simulant's total oxygen mass content [64]. Moving from theoretical process studies to practical application, regolith extraction technologies must soon undergo comprehensive engineering and operational testing within the specific constraints of the lunar environment. Importantly, lunar gravity may not be enough to ensure separation of oxygen bubbles from the anode [65]. Validation in relevant environments is the next necessary step to consolidate extraction technologies [66]. The byproduct of these processes is particularly rich in a mixture of structural metals, including iron, titanium, and aluminum, making it potentially suitable to be used for the in situ manufacturing of tools or basic infrastructure elements [67]. Current research on lunar construction based on local materials is oriented toward evaluating properties such as mechanical strength and durability, as well as production technologies such as 3D printing.

KREEP is not a single mineral phase, but a geochemical signature expressed across multiple lithologies, including basalts, impact melts, breccias, and regolith fines. It reflects enrichment in potassium present mainly in feldspathic and glassy phases; Rare Earth Elements, with 15 lanthanides (La-Lu), Y and Sc, and phosphorus (P) concentrated in accessory phases such as phosphate minerals and glasses. Due to their formation process as a geochemical residue of the late-stage crystallization of the Lunar Magma Ocean (LMO) [67], KREEP signatures are not uniformly distributed across the Moon. The NASA Lunar Prospector and subsequently the Japan Aerospace Exploration Agency (JAXA) Kaguya missions showed that KREEP-rich materials are strongly concentrated in the Procellarum KREEP Terrane (PKT) on the lunar near side, spatially correlated with high Th and U abundances [68]. Understanding KREEP distribution improves models of lunar differentiation and crustal evolution. While KREEP components are traditionally viewed as the final residual ~0.5% of LMO, their localized enrichment within the so-called "red spots" suggests a potential origin through extreme fractional crystallization of basalt-underplated crust or secondary remelting of KREEP-rich lithologies triggered by major impact events [69]. Red spots are silicic, non-mare volcanic constructs of 1–10 km size with high Th abundance, appearing as high-albedo domes or plains in the surrounding dark mare basalts; hence, their identification is possible by multispectral mapping and UV–visible spectroscopy, as well as thermal radiometry and radar [70]. REE concentrations associated with the KREEP-rich silicic nature of lunar red spots make them promising exploration targets, though their characterization as ore deposits remains premature, pending direct sample analysis. The origin of KREEP basalts was extensively debated in the scientific community, largely based on the analysis of returned samples by the Apollo 14 and 15 [71].

From an ISRU perspective, KREEP materials are not direct-use consumables, but they represent a strategic, process-dependent resource with potential long-term value for export to Earth, where REEs are critical for electronics, magnets, energy systems, and

advanced manufacturing. While terrestrial REEs are abundant, their supply chains are geopolitically constrained, and their processing involves serious environmental hazards due to the chemical nature of the minerals, the extraction methods, and the refining processes that cause water pollution with heavy metals and general chemical spills. Hence, lunar REEs could become relevant for future component manufacturing established directly in the lunar environment, with the products either used in situ or exported to Earth. Phosphorus and potassium are both essential for biological systems, making them potentially suitable for bioregenerative life support systems, chemical processes, and plant growth systems. Furthermore, KREEP materials may be of interest for future commercial metal smelting and extraction operations, although the required refining technologies are presently at a low level of maturity and suffer from high energy demand. Conversely, KREEP-rich basalts offer a promising potential for construction material manufacturing; their enrichment in incompatible elements depresses their solidus and liquidus temperatures [72], which could facilitate lower-energy thermal sintering or casting into bricks and radiation shielding structures compared to highland anorthositic regolith.

Radioactive elements including thorium (Th) and uranium (U) are typically associated with KREEP terrains as a result of late-stage magmatic processes. This co-presence provides an opportunity for the indirect detection of KREEP via [59,73]. A global lunar map of U distribution, made possible by exploiting measurements from the Kaguya orbiter, revealed significant variations in U/Th on the far side [74]. The future of KREEP prospecting on the lunar surface through indicators, notably, the radioactive elements, will require improved spatial resolution (<100 m) for orbital mapping instruments, as well as, more importantly, in situ direct measurements. Considering metal extraction as potential ISRU technology in support of construction [75], the distribution of Titanium and Iron in the common forms of TiO_2 and FeO, respectively, has been mapped since the first orbital mission [58,76,77] and it remains among the most relevant achievements of recent lunar prospecting and surface mapping [78]. Removing the Fe and Ti contributions from the Lunar Prospector Neutron Spectrometer (NS) data, these were used in [79] to isolate primarily REE contributions from gadolinium (Gd) and samarium (Sm) as high-precision proxies. Thermal neutron measurement was subsequently confirmed as an additional technique to map the enrichment of these incompatible elements [80]. Complementing orbital observations, in [81], the authors used in situ VNIS spectra from the Yutu-2 rover to generate fine-scale FeO and TiO_2 abundance maps of the lunar far side, demonstrating the value of high-resolution surface spectroscopy for resolving compositional heterogeneity beyond the reach of orbital instruments.

3. Scientific Measurements Enabling Resource Assessment

Various measurement techniques and related instruments for remote sensing and in situ investigations have been developed by researchers and engineers since the beginning of the space science era, initially to observe Earth, and subsequently other celestial bodies. The payload of planetary probes includes a large variety of equipment, sometimes derived from laboratory concepts, operating in particularly harsh environments while maintaining high performance and reliability. Although primarily designed to achieve scientific objectives, their datasets have also been processed with the aim of informing reliable resource prospecting.

Mineralogical and elemental mapping are certainly the key foundations for assessing the chemical potential of lunar surface materials, identifying and quantifying target resources for future ISRU. A very recent comprehensive review of remote sensing and surface-based prospecting, mapping and materials characterization technologies for the Moon is contained in [82], which also offers valuable insights into downstream elements of the value chain, from resource acquisition and transportation to infrastructure

construction. In addition to compositional characterization alone, evaluating the physical state and surface exposure history of the lunar regolith is equally critical for effective resource prospecting and ISRU planning. In this context, geotechnical and optical parameters such as grain size distribution (initially inferred at large scale through remote sensing observations of surface physical properties and then validated and refined through in situ ground-truth measurements) and surface maturity, quantified via the Optical Maturity (OMAT) index introduced in [83], strongly influence regolith mobility, thermal conductivity, and the overall feasibility of ISRU processing. However, while acknowledging the importance of these factors, the remainder of this work primarily focuses on the characterization of compositional aspects of resource prospecting.

In the following sections, a systematic examination of the most relevant techniques for lunar prospecting is reported, organized into distinct classes of instruments operated during exploration missions over the last few decades. Such payloads were generally hosted on board orbiters, for large-scale observation and lunar surface mapping, or on surface platforms (e.g., landers and rovers) when a ground truth was deemed necessary. Integrating these complementary datasets is essential for reconciling topographical patterns with microscopic material properties, thereby enabling a more comprehensive understanding of lunar environments [84]. For each measurement technique, a concise description of its underlying measurement principle is followed by selected examples of payloads flown on past or active missions; its applications in resource prospecting are then elaborated, highlighting its respective strengths, limitations, and potential mitigation strategies.

3.1. Visible Imaging

Visible-light cameras are among the most indispensable tools for planetary exploration, especially during the early studying of a destination. Both in single and paired configuration, they allow reconstruction of morphological, albedo, color and illumination-context maps at resolutions from hundreds of meters to the sub-meter scale, supporting geological context determination and assessments on surface evolution, volcanic and tectonic processes. Considering their versatility, there are embarked on many of the exploration science orbital or surface probes.

In the modern era of lunar mapping, the JAXA Kaguya orbiter operated the Terrain Camera (TC), a dual-head stereo visible imager operating at about 10 m/pixel spatial resolution, designed to generate monochromatic high-resolution tiled frames and mosaics. It also enabled the generation of a global and extremely uniform lunar Digital Elevation Model (DEM), whose vertical accuracy is improved using more precise data from instruments, such as Kaguya's laser altimeter, for alignment and correction. TC data revolutionized lunar topography by revealing detailed basin structures, volcanic activity evidence [85], tectonic features, and polar illumination conditions. Shadow analyses allowed the identification of a 65 m diameter vertical hole in the Marius Hills region of the Moon, which was interpreted as a skylight of an intact lava tube [86]. In the same timeframe, the first Chinese lunar orbiter Chang'e-1 carried a three-line-array Charge-Coupled Device (CCD) imaging system operating in the visible range with a spatial resolution of ~120 m, producing China's first global lunar DEM. While relatively modest in resolution, these data contributed an independent topographic reference and supported large-scale geological interpretations [87]. The Terrain Mapping Camera (TMC) on ISRO Chandrayaan-1 was a push-broom stereo imager operating in the visible–near-infrared range used to generate high-resolution three-dimensional maps of the Moon. It provided near-global topographic coverage and significantly improved knowledge of lunar slopes and roughness [88], contributing to chemical, mineralogical and topographic mapping of the lunar surface at high spatial resolution. The signal-to-noise ratio (SNR) was also significant at

the poles and in the mid-latitude regions for mature mare soil, which is one of the darkest areas on the lunar surface. Although not a compositional instrument, TMC data were combined with hyperspectral images and X-ray fluorescence measurements, to support the lunar surface composition assessment [89]. As part of the payload of the ISRO Chandrayan-2 orbiter, TMC-2 was a follow-on of the TMC, configured to acquire panchromatic images and stereo triplets from a 100 km circular orbit around the Moon for preparation of a detailed three-dimensional map or DEM of the complete surface. Recent advancements in deep learning and machine learning techniques applied to lunar crater detection maximized the return of TMC-2 data [90]. State-of-the-art, high-resolution spatial datasets of the lunar surface are provided by the Narrow Angle Cameras (NACs), which form the NASA Lunar Reconnaissance Orbiter Camera (LROC) payload together with the Wide Angle Camera (WAC). The WAC is a 7-color push-frame camera (100 and 400 m/pixel visible and UV, respectively), while the two NACs are monochrome narrow-angle linescan imagers producing ~0.5 m/pixel panchromatic images (over 5 km swath at ~50 km altitude) and a wide angle camera (WAC) delivering 7-band UV/visible multispectral images at ~100 m/pixel over a ~60 km swath [91]. LROC data are widely used for characterizing surface hazards, illumination conditions, and small-scale geomorphology, making the instrument a cornerstone for all the context information in support of surface activities [92]. The high-resolution NAC images have been used to generate detailed topographic maps via stereo or photometric stereo analyses, illuminating subtle surface features (faults, small craters, tectonic or collapse structures) that inform crustal evolution studies and facilitates identification of surface compositional provinces. The continuous imaging of polar and near-polar regions has allowed mapping of illumination and shadow patterns over lunar seasons, essential information for understanding thermal environment, regolith illumination history and planning future missions or long-lived landers/settlements [93]. The generation of accurate and comprehensive DEMs of planetary surfaces often implies the combination of high-resolution horizontal views captured by cameras, also in stereo configuration, with the absolute vertical reference illumination-independent framework measured through orbiter laser altimeters. Before the fusion, data could be potentially acquired by different missions, for example in the case of the co-registration of 43,200 DEM tiles generated by Kaguya TC to the NASA LRO Lunar Orbiter Laser Altimeter (LOLA) geodetic framework, producing a combined topographic map of the Moon at a resolution of 512 pixels per degree (corresponding to ~60 m at the equator) [94].

Cameras operating in the visible range are also embarked on surface elements including landers and especially rovers; even in this case, the main purpose of these instruments is to collect information on local surface features and morphology (often, with geological implications) and, in general, to provide context scenario, this time at local scale. Cameras provide a critical source of data to support optical navigation during the pinpoint accurate landing phase, in addition to laser and radar altimeters and inertial sensors [95]. Similarly, cameras on mobile elements feed the data fusion terrain navigation systems for traverse planning and execution in an unknown environment. Significant recent examples include the Panoramic Camera (PCAM) on the Chinese Chang'e-3 mission, a stereo visible imager providing centimeter-scale topography for obstacle avoidance and traverse planning, and also allowing evaluation of photometric properties of the landing site, used to infer regolith maturity and physical state [96].

Even though orbital and surface visible imagery instruments are widely adopted on all the exploration platforms because of their basic functions and versatility, they do not offer direct surface compositional or subsurface structure insights. Their limitations in directly informing resource prospecting are mainly due to their lack of spectral specificity. In fact, visible albedo/color differences can hint at lithologic differences but rarely suffice to discriminate minerals or to identify volatile-bearing regolith. Moreover, camera

performances are strongly impacted by illumination conditions. Thus, surface visible imaging serves as a first-pass reconnaissance and contextualization tool for the scientific investigation as well, but it is not by itself appropriate for resource identification or quantification on the Moon. Nevertheless, this technique plays an indirect but important role in building knowledge and providing indirect information. Morphological mapping reveals features, notably surface structures, lava flows, pyroclastic deposits, geologic unit boundaries, and crater ejecta features, that may correlate with buried stratigraphy, depth variation, or exposures of fresh material. Such features are prime targets for more detailed resourcing follow-up, usually via in situ measurements by spectrometry, or subsurface drilling and analysis [39,97,98]. Topography is essential for identifying permanently shadowed regions and assessing thermal and illumination environments favorable to volatile stability [99]. Albedo variations across terrains can highlight different lithologies, helping to locate regions with higher resource potential. Imaging of permanently shadowed regions, slopes, and terrain hazards is essential for planning safe landings or rover traverses aimed at volatile hunting. Visible imagery also provides the base context for thermal, neutron, or radar data, aiding selection of candidate sites for volatiles or ore exploration.

3.2. Spectrometry

This technique is based on the acquisition of spatially resolved reflectance spectra across contiguous spectral bands, producing image cubes where each pixel contains a full spectral signature used to discriminate between minerals and volatiles on planetary surfaces. In lunar exploration, visible–near-infrared (VNIR) and shortwave infrared (SWIR) imaging spectrometers are traditionally used to measure the reflected portion of sunlight illumination in the specific bands, to detect spectral absorption features of the minerals distributed on the surface of the Moon.

A milestone unit of this family of instruments was the M^3, a VNIR imaging spectrometer spanning ~0.43–3.0 μm that provided the first high-resolution global hyperspectral dataset of the lunar surface, revealing mineralogical diversity and signatures of OH/H_2O absorption bands near 3 μm. Its grating-based design achieved ~10 nm spectral sampling and ~70 m spatial resolution in target mode, enabling mineral classification and baseline compositional mapping for future exploration and resource assessment. Such comprehensive spectral coverage demonstrated the viability of hyperspectral imaging for detecting hydration and silicate mineralogy [40], forming a baseline for subsequent missions [100,101].

Building on M^3 heritage, the Chandrayaan-2 Orbiter was equipped with the Imaging Infrared Spectrometer (IIRS), observing the Moon surface in the range from ~0.8 μm to ~5.0 μm with ~250 contiguous spectral bands and ~80 m spatial resolution. It extends spectral coverage into the mid-infrared to better resolve hydration features near 3.0 μm and other mineral absorptions. IIRS's hyperspectral cubes support improved discrimination of mineral and volatile phases across the lunar surface under varying illumination conditions, advancing regional mineral mapping capabilities [102].

Spectrometry is also widely used as scientific payload on surface probes, obtaining compositional data of limited regions but with higher performances, complementing information obtained on a larger scale by orbital observations. The Visible and Near-Infrared Imaging Spectrometer (VNIS) instruments aboard the Yutu and Yutu-2 rovers of the Chinese Chang'e-3 and -4 missions, respectively, provided in situ imaging spectrometry over ~0.45–2.4 μm using acousto-optic tunable filters [103]. This technique enabled direct compositional measurements of regolith and rocks along rover traverses at high spatial and spectral resolution, validating orbital datasets and revealing local variations in iron and titanium abundances on the far side of the Moon [104,105]. A few years later, the Lunar Mineralogical Spectrometer (LMS) was used during Chang'e-5 mission to support

the characterization of the locations where the samples were acquired. Covering ~480–3200 nm with hundreds of bands and high spectral resolution, it allowed fine-scale mineralogical discrimination and detection of OH/H_2O at sampling sites. LMS scanning capabilities and integrated calibration units enhance quantitative reflectance measurements critical for characterizing local resource potential and contextualizing returned samples [106].

Spectrometry in the range of thermal infrared (TIR), a well-established technique in Earth and planetary science, measures the emitted planetary heat, revealing atmospheric and surface composition, and, potentially, resource distribution. The Diviner Lunar Radiometer Experiment (DLRE) onboard NASA LRO has been acquiring solar reflectance and mid-infrared radiance measurements across a wavelength range of 0.3 to 400 μm and 9 channels. Its extensive and complete mapping of the lunar surface provided a comprehensive view of the thermal state of the near-surface layer of the Moon at 0.5° resolution, allowing the understanding and accurate modeling of the thermal behavior of the lunar regolith, depending on its composition and status [107]. During an Earth gravity assist maneuver performed in 2022, the NASA probe Lucy (designed to study Jupiter's Trojan asteroids) pointed the Thermal Emission Spectrometer (LTES) instrument to the Moon surface and acquired hyperspectral thermal infrared observations of the Oceanus Procellarum [108]. These data represent the first well-calibrated high-spectral-resolution TIR observations of the Moon, covering 100–1750 cm^{-1} (100–5.8 μm) at a spectral sampling of 8.64 cm. An upgraded version of the Diviner instrument was embarked on the Lunar Trailblazer smallsat: the Lunar Thermal Mapper (LTM) is a 15-channel multispectral infrared radiometer that covers a range between 6 and 100 μm. LTM advances infrared compositional analysis by incorporating eleven narrowband compositional filters across the 6.25 to 10 μm range, enabling more precise characterization of key features [109]. The instrument could not observe the Moon since the Lunar Trailblazer satellite, after the launch in 2025, did not enter operations. To complement photometric, spectral and thermophysical characteristics, the PolCam on board the Korea Pathfinder Lunar Orbiter (KPLO) or Danuri Korean orbiter is completing a quantitative mapping of polarimetric anomalies of the lunar regolith. Polarization of solar light scattered by regolith depends on optical (refraction index, transparency) and geometric (particle size, surface roughness) properties, both controlled by the regolith composition and strongly affected by space weathering [110].

In the search of the most promising regions for ISRU, imaging spectrometers provide global and regional hyperspectral datasets and allow the generation of spatially resolved compositional maps across broad areas, enabling the identification of minerals and hydration features that indicate volatile reservoirs and resource-bearing materials. In addition, in situ spectrometers offer high spectral resolution and ground-truth validation, essential for refining orbital interpretations and quantifying local resource abundance, including subtle OH/H_2O bands.

Nevertheless, imaging spectroscopy alone does not directly quantify elemental abundances and does not inform on subsurface resources presence. Orbital instruments are limited by spatial resolution and surface illumination conditions, which can complicate detection of fine-scale resource heterogeneities and shadowed terrain spectral interpretation. Even in the case of extended spectral range, discerning low-abundance hydration signatures remains challenging in mixed terrains. In situ instruments are constrained by traverse range and cannot provide global coverage, requiring complex integration with orbiting datasets. This technique must be then integrated with other measurements (e.g., XRS, NS, radar) for comprehensive resource characterization. The combination of orbital hyperspectral mapping, in situ spectral measurements, and auxiliary datasets creates a robust framework for potential resource detection [111]. Orbital imaging spectrometry

identifies broad compositional trends and volatile indicators, while in situ spectrometry confirms local mineralogy with high precision and supports quantitative interpretation, crucial for ISRU assessment and mission planning. This hierarchical data synergy enhances the ability to locate and evaluate lunar resources such as water-bearing minerals and essential elements.

3.3. Gamma-Ray Spectrometry

Gamma-ray spectrometry (GRS) is a well-established measurement technique for determining the elemental composition of the surface of airless planetary bodies. On the Moon, gamma rays are primarily produced through interactions between galactic cosmic rays and the upper layers of the regolith, generating characteristic nuclear emissions via inelastic scattering, neutron capture and radioactive decay. Each element emits gamma rays at discrete energies, allowing quantitative determination of major, minor, and trace elements such as iron (Fe), titanium (Ti), aluminum (Al), silicon (Si), calcium (Ca), magnesium (Mg), potassium (K), thorium (Th), and uranium (U) from orbit [112]. The effective sampling depth of lunar gamma-ray measurements is typically on the order of 10–30 cm, corresponding to the penetration depth of cosmic-ray-induced secondary particles, making the technique directly sensitive to bulk regolith composition rather than surface coatings. Instrument performance is governed by detector material, energy resolution, orbital altitude, and integration time, resulting in spatial footprints ranging from tens to several hundreds of kilometers. While this relatively coarse spatial resolution limits site-scale discrimination, gamma-ray spectrometry uniquely provides absolute elemental abundances that are difficult or impossible to obtain with optical or infrared methods alone [113].

GRSs flew on the majority of the lunar orbiters, especially the ones operating in the first decade of this century (e.g., Kaguya, Lunar Prospector, Chandrayaan-1, Chang'e-1 and 2), with the aim of achieving a global map of element distribution, the identification of large-scale geochemical provinces, investigating the composition and thickness of the lunar crust. They also provided key evidence for the heterogeneous distribution of heat-producing elements, data critical to refining models of lunar differentiation, magmatic evolution, thermal history and element migration [114]. From an applied perspective, gamma-ray spectrometry plays a critical role in resource assessment by directly quantifying elements relevant to in situ resource utilization, including iron, titanium, and thorium, as well as constraining the oxygen extraction potential of the regolith. For resource prospecting, this technique offers the unique strength of providing direct, quantitative measurements of elemental abundances in the lunar regolith, independent of illumination conditions and largely insensitive to surface maturity or space-weathering effects. GRSs can probe the upper tens of centimeters of the regolith, yielding bulk compositional information that is directly relevant to in situ resource utilization, particularly for the assessment of metal-rich materials such as Fe- and Ti-bearing basalts. These measurements are also globally consistent and absolute in nature, enabling robust identification of large-scale geochemical provinces and reducing ambiguities inherent to purely spectral or morphological methods. Datasets identified the regions with higher KREEP abundance, constraining both the Moon's differentiation and the distribution of trace elements of potential economic interest; this was mainly possible using Thorium as an indirect indicator of KREEP presence [73,115]. The GRS onboard Chang'e-2 allowed the creation of a potassium distribution on the Moon, coherent with previous observations; it was found in abundance in the Mare Crisium and Mare Orientale, suggesting possible basin-forming impacts that excavated material from deep layers up to the lunar surface [116]. However, raw data are affected by various factors such as solar activity, deep space environment, cosmic rays and satellite operations; hence, a rigorous reduction and correction process is

necessary for reliable measurement and data interpretation, as necessary for the KPLO data [117].

To date, the only gamma-ray-sensitive instrument operated at the lunar surface (specifically, at the SPA basin, at the far side of the Moon) was the Lunar Lander Neutrons and Dosimetry (LND) of the Chang'e-4 mission [118]. Designed for measurements of doses, it can also detect fast neutrons generated by the regolith after impingement by high-energy particle radiation and thermal neutrons as indicators of subsurface water, but was not capable of providing compositional info of the Moon.

Although measurements of this nature cannot directly detect water or volatile species, they provide an indispensable geochemical framework that, when combined with neutron spectrometry and high-resolution imaging, underpins modern lunar resource exploration strategies. However, these strengths are counterbalanced by a few limitations: the intrinsically low gamma-ray flux requires long integration times and results in coarse spatial resolution from orbital platforms, which severely limits the technique's applicability for site-specific resource targeting. GRS is fundamentally insensitive to volatile species such as water and hydroxyl, making it unsuitable as a standalone tool for polar resource prospecting. Furthermore, the interpretation of elemental abundances can be affected by regolith mixing, compositional heterogeneity at sub-footprint scales, and uncertainties in cosmic-ray flux variations. Consequently, while GRS is indispensable for establishing regional-scale resource potential and compositional baselines, it must be complemented by higher-resolution imaging, NS, and in situ measurements to support operational ISRU decision-making [119].

3.4. X-Ray Spectrometry

X-ray spectrometry (XRS) represents a cornerstone technique for the geochemical characterization of planetary surfaces, enabling the precise identification and quantification of major rock-forming elements. This analytical method relies on the interaction between high-energy incident radiation (typically from solar X-rays or onboard radioactive sources) and the atomic structure of the lunar regolith. When an atom is excited, it emits secondary X-rays at characteristic energy levels, a phenomenon known as X-ray fluorescence (XRF), which serves as a definitive spectral fingerprint for elements such as aluminum (Al), magnesium (Mg), silicon (Si), calcium (Ca), iron (Fe), and titanium (Ti) [112]. In planetary science, the application of X-ray spectrometry depends on mission architecture; from orbital platforms, XRS operates as a remote sensing tool, using the Sun as a natural excitation source to map regional elemental abundances. Conversely, for in situ applications, the technique can be adopted using internal excitation sources; hence, such an active instrument allows researchers to achieve millimetric spatial resolution to execute chemical analyses of rocks and soil at a micro scale, independent of solar activity.

X-ray measurements are sensitive to the extreme surface layer of the regolith, typically probing only the upper few micrometers to tens of micrometers, as dictated by the shallow penetration depth of both incident solar X-rays and emitted fluorescent photons. Consequently, XRS directly reflects surface composition rather than bulk regolith properties. Instrument performance and data quality are strongly dependent on solar illumination conditions, detector efficiency, and viewing geometry, resulting in spatial resolutions that can reach a few tens of kilometers from orbit under favorable conditions but degrade significantly during periods of low solar activity [120]. XRSs have been flown on several lunar missions, including Apollo 15 and 16, Kaguya, Chandrayaan-1, Chang'e-1, and Chang'e-2, enabling the creation of near-global maps of major elemental abundances. These datasets have been instrumental in distinguishing lunar terrains, characterizing mare basalt compositions, and refining models of crustal differentiation and magmatic evolution. Specifically, X-ray data provided key constraints on the global distribution of

FeO and TiO_2, contributing to the identification of major geochemical provinces and compositional gradients across the lunar surface [121]. From an applied perspective, X-ray spectrometry contributes to lunar resource assessment by constraining the surface abundance of elements directly relevant to in situ resource utilization, especially iron- and titanium-bearing phases associated with mare basalts and oxygen extraction potential.

In situ X-ray spectrometry applications date back to the Alpha Scattering Experiment (APXS) on the Surveyor landers and the Roentgen Isotopic Fluorescent Method of Analysis (RIFMA) XRF instrument on the Soviet Lunokhod rovers. More recently, the APXS onboard the Chinese Yutu rover of the Chang'e-3 mission [122], using the radioactive sources ^{55}Fe and ^{109}Cd decay to produce particles and X-rays, has provided high-resolution chemical assays, reinforcing X-ray spectroscopy as a primary tool for validating orbital geochemical maps.

An extremely effective in situ use of X-ray diffraction is exploited in the X-ray diffraction (XRD) instrument, currently the most powerful tool to determine the nature of crystalline phases and the atomic structure of geological materials. The design of XRD for planetary applications is challenging, due to the required mechanical stability and precise optical alignment. To date, the only XRD operated for space exploration was part of the Chemistry and Mineralogy suite onboard the NASA Mars Science Laboratory (MSL) rover Curiosity; since early operation, relevant achievements were enabled in mineralogy definition of the landing site, i.e., Gale crater on the planet Mars [123]. However, no XRD has operated on the lunar surface yet.

The X-ray spectroscopy is particularly valuable for identifying compositional endmembers, mapping high-Ti regions, and providing ground truth for mineralogical interpretations derived from optical and infrared spectrometry. Its sensitivity to major elements makes it a robust tool for regional-scale compositional characterization, supporting the selection of candidate areas for further exploration and follow-up investigations. Conversely, XRS also presents a strong dependence on solar X-ray flux, which restricts data acquisition to sunlit regions and introduces temporal variability complicating quantitative interpretation. For mitigation, sources of X-ray are studied to obtain active XRSs for orbiters or rovers [124]. Moreover, the shallow sampling depth makes the technique sensitive to surface maturity, space-weathering effects, and regolith gardening, which may decouple surface composition from subsurface materials relevant for ISRU. Furthermore, XRS is inherently insensitive to volatile species, and trace elements present at low abundances, limiting its standalone applicability for resource prospecting. Consequently, while XRS provides high-value compositional constraints on the lunar surface, it is most effective when integrated with GRS, NS (see Section 3.5), and infrared observations to establish a coherent and multi-scale framework for lunar resource exploration [113]. The regolith physical properties (grain size, roughness, porosity) also affect fluorescence yields and consequently the performances of this measurement technique; as described in [125], laboratory characterization campaigns demonstrated that the particle size effect in XRF cannot be neglected and should be corrected for quantitative major elemental analysis, especially when observed at large phase angles. Additional limitations are due to the overlapping of soft X-ray spectral lines from adjacent elements, complicating deconvolution; technologies such as higher-resolution Silicon Drift Detector (SDD) and advanced pulse processing algorithms can improve line separation and quantification. The capability to observe beyond the first layer of regolith can be extended by combining XRF with deeper-penetrating techniques (e.g., GRS and NS) and with in situ sampling and analyzing.

3.5. Neutron Spectrometry

Neutron spectrometry (NS) is a remote-sensing technique widely used to investigate the elemental composition and volatile content of airless planetary bodies. On the Moon,

neutrons are generated when galactic cosmic rays interact with atomic nuclei in the upper layers of the regolith, producing cascades of secondary neutrons through spallation reactions. These neutrons undergo elastic and inelastic scattering and are progressively moderated before escaping the surface. Their energy distribution (commonly classified into fast, epithermal, and thermal neutrons) is strongly controlled by the presence of hydrogen, which is highly efficient at slowing neutrons through elastic collisions. As a result, neutron spectrometry is uniquely sensitive to hydrogen abundance in the shallow subsurface, making it a primary technique for the detection and mapping of hydrogen-bearing materials on the Moon [36].

The effective depth of neutron measurements extends to approximately the upper meter of the regolith, with sensitivity increasing with depth for epithermal and fast neutrons compared to gamma-ray techniques. Orbital neutron spectrometers typically achieve spatial resolutions ranging from tens to several hundreds of kilometers, depending on detector design, orbital altitude, and integration time. Although coarse in spatial scale, neutron spectrometry provides a direct, physically grounded proxy for hydrogen concentration that is largely independent of surface illumination and optical properties [37].

The energy distribution and count rates of these neutrons carry signatures of the subsurface composition, particularly hydrogen abundance, since in the fast neutron energy range there is a linear relationship between the neutron flux and average atomic mass of elements in the lunar regolith [126]. In order to increase the sensitivity of the measurement, the use of a Pulsed Neutron Generator (PNG) was proposed in [127] recently, together with the expected benefits in distinguishing hydrogen-rich materials from enrichments in thermal neutron-absorbing elements including gadolinium (Gd), samarium (Sm), and europium (Eu).

NSs flown on missions such as Lunar Prospector, Kaguya, Chandrayaan-1, Chang'e-1 and Chang'e-2 have enabled creation of the first global maps of hydrogen distribution on the Moon. These datasets provided evidence for enhanced hydrogen concentrations at high latitudes, particularly within PSRs, supporting the presence of water ice or hydrogen-rich compounds trapped in cold environments. At lower latitudes, neutron data reveal a more diffuse and lower hydrogen background, consistent with solar wind implantation and transient surface hydration rather than stable water reservoirs [128].

The Chang'e-4 LND, the first of its kind on the surface, provided measurement of fast and thermal neutrons, both for the characterization of the radiation environment in view of future human exploration, and for the quantification of subsurface water content in the SPA basin [118]. Energetic neutral atoms (in the range from 10 eV to 10 keV) were captured by the Advanced Small Analyzer for Neutrals (ASAN), part of the scientific payload of the Chang'e-4 Yutu rover [129]. Developed in a cooperation between Swedish and Chinese research institutes, it allowed the identification of neutral hydrogen, helium, and the oxygen group.

Water is certainly the most interesting resource that can be indirectly quantified by neutron spectrometers, through the measurement of the depth-dependent distribution of hydrogen, a few tens of cm down in the lunar terrain [130]. The detection of epithermal-neutron suppression is interpreted as hydrogen enrichments suggestive of water ice. Recent hydrogen mapping by the Lunar Exploration Neutron Detector (LEND) of the NASA LRO focused on polar regions, while also comparing to equatorial ones and model predictions [131]. Multiple observations of the permanently shadowed region Cabeus-1 in the vicinity of the lunar south pole allowed quantification of hydrogen, estimated to be 0.49 ± 0.05% by mass fraction, with a peak of about 0.7% at the very bottom of the crater [132], in line with LCROSS impact experiment results.

From an applied perspective, neutron spectrometry plays a central role in lunar resource assessment by providing the most direct orbital constraint on hydrogen abundance, a critical proxy for water and other volatiles relevant to in situ resource utilization. For polar exploration, neutron data underpin the identification of candidate volatile-rich regions and inform landing site selection and mission architecture for ISRU-focused missions. When combined with thermal models, illumination conditions, and topographic data, neutron spectrometry enables first-order discrimination between transient surface hydration and more stable subsurface volatile accumulations.

Despite these strengths, NS presents several limitations; the technique does not distinguish between different hydrogen-bearing species, such as hydroxyl, water, or hydrated minerals, and therefore cannot independently confirm the physical state or extractability of detected hydrogen. Spatial resolution from orbit remains coarse, limiting its utility for site-scale resource characterization and necessitating follow-up observations at higher resolution or in situ. Additionally, neutron fluxes are influenced by regolith composition, density, and cosmic-ray variability, introducing uncertainties that require precise modeling and crosscalibration with gamma-ray data. Consequently, NS is best-suited for regional-scale volatile prospecting and must be integrated with GRS, IR, and surface measurements to support robust and operationally relevant lunar resource exploration strategies [119].

3.6. Radar

Radar remote sensing is extensively utilized in planetary science, allowing for characterization of subsurface morphology and composition of rocky bodies [133]. One of the typical design trade-offs is the one comparing penetration vs. resolution: deeper penetration sacrifices vertical resolution; conversely, higher-frequency channels image shallow (~tens of meters) but with better resolution. In lunar science, this trade-off is reflected in two instruments: orbital synthetic aperture radar (SAR), where the orbital motion of the satellite itself is used to virtually enlarge the size of the radar antenna, and ground-penetrating radar (GPR), deployed on surface platforms to operate in situ.

Radars in the SAR configuration operating on board orbiters allow for studying of planetary surfaces and subsurfaces due to the sensitivity to the roughness, structure and composition of the surface material and its ability to penetrate the surface to reveal the buried terrain features [134]. SAR is particularly effective for characterizing lunar pyroclastic deposits: because radar waves can penetrate the surface, they can reveal buried lava flows and crater ejecta units beneath the mantling material. Radar can also be used to assess the locations of the thickest parts of pyroclastic deposits and to distinguish fine-grained pyroclastic material from optically dark mare regions. Polarimetric and multi-frequency SAR can help distinguish between rough blocky terrain and materials with lower dielectric constants such as water ice. Hosted on the ISRO Chandrayaan-1 orbiter, the polarimetric Mini-SAR operated in S-band only (~12.6 cm). It mapped permanently shadowed regions at both poles, producing high values of Circular Polarization Ratio (CPR) that were interpreted as possible indicators of water ice in some crater interiors, though high CPR can also originate from blocky terrain. As a technology demonstration, Mini-SAR laid groundwork for more advanced radar polarimetry [135,136]. Dual-Frequency SAR (DFSAR) on Chandrayaan-2 Orbiter utilizes L- and S-band SAR with polarimetric modes to disambiguate scattering mechanisms and improve discrimination of potential near-surface ice deposits in polar shadowed zones and characterize scattering from different terrains, allowing also the evaluation of lunar surface roughness [137,138]. Dual frequencies allow estimation of near-surface dielectric parameters and help separate roughness effects from volumetric scattering that could be associated with ice. Mini-RF on LRO, the successor to Chandrayaan-1 Mini-SAR, was designed with both S-band (~12.6

cm) and X-band (~4.2 cm) capabilities and performs polarimetric radar observations to investigate potential water ice deposits and surface roughness anomalies at polar craters. Analyses of Shackleton crater's interior suggest only a few percent of patchy ice mixed with regolith, requiring careful interpretation due to surface geometry effects [139,140].

Compared to SARs, GPRs exploit lower frequencies and ground-coupled antennas to image subsurface stratigraphy, with penetration depth and resolution governed by frequency, antenna configuration, and regolith electrical properties. This technique is essential for revealing buried layering and dielectric contrasts down to tens or hundreds of meters, complementing surface spectroscopic and orbital observations. Both Yutu and Yutu-2 Rovers of Chang'e program hosted surface GPR systems with dual channels named Lunar Penetrating Radar (LPR). On Yutu, LPR provided the first rover-based subsurface stratigraphic scans to ~30 m depth (enabling insights into regolith and buried layering) [141,142]. A few years later, LPR on Yutu-2 imaged multiple subsurface layers down to ~100 m or more beneath the far-side landing site, revealing stratification of ejecta and mare sequences and allowing estimates of layer thickness and dielectric contrasts that inform regolith structure [143,144]. The highest resolution in radar data to date was obtained by the Chang'e 5 Lunar Regolith Penetrating Radar (LRPR) (the first operated array of GRP); the data revealed the complexity of the interior structure of the shallow regolith of the Moon, that consists of ejecta from different craters that occurred over time. The Chang'e 5 radar observations reached up to ~2.5 m of the subsurface, and revealed a strong capability to absorb electromagnetic waves, suggesting a relatively high $FeO + TiO_2$ content within the lunar regolith [145,146]. Notably, upcoming Chinese missions of the Chang'e program, such as Chang'e 7 and Chang'e 8, will all carry GPR systems similar to that of Chang'e-5; of particular significance, the Chang'e-7 mission is slated to land at the lunar south pole, presenting an opportunity to utilize the GPR to detect water ice.

For resource identification and distribution, radars are particularly suitable in the creation of a context set of information related to the planetary subsurface, extending the detecting capability of all the other instruments beyond the first layer of terrain. Moreover, the knowledge of the relative permittivity distribution and its contribution to radar surface scattering is essential for the identification of volatiles and their nature, making this technique the best-fit technique currently available to detect these resources. SAR polarimetry at multiple bands l (e.g., Chandrayaan-2 DFSAR) can constrain dielectric properties of surface and near-surface materials, potentially discriminating between dry regolith and mixtures containing ice or volatiles [147,148]. Crater interiors in PSR in the polar regions shown anomalously high CPR, most probably resulting from various factors such as presence of volatiles, crater morphology, e.g., wavelength scale roughness and slope, shape of the rocks and orientation of the buried rocks [149]. The combination of the data acquired by the three main SARs sensing the Moon and the application of different decomposition techniques allowed dielectric characterization and polarimetric analysis, indicating the presence of surface ice clusters in the crater's walls and on some areas of the crater floor [150].

GPRs on board rovers provide direct layering information and dielectric contrasts at scales inaccessible to orbiters, offering ground truth for subsurface structure including buried layers that may influence volatile trapping or mechanical properties relevant to ISRU. The in situ helium-3 reservoir at the Chang'e-3 landing site was indirectly estimated by the Yutu high-frequency radar to measure surface content of TiO_2, and then combined with the relationship between TiO_2 content and the concentration of helium-3 established from Apollo regolith sample analyses [151]. In the future upcoming mission of China's lunar exploration program Chang'e-7, an upgraded version of LPR will be installed on the rover [152], equipped with both high-frequency and low-frequency channels, and,

based on a pseudo-random coding system, it will allow detection of subsurface stratification and identification of water ice.

Exploitation of radar data usually requires an intense effort and advanced processing to separate true subsurface features from noise and antenna effects; it also implies difficulty distinguishing real targets from artifacts. Multiple reflections can mimic geological layers, leading to misinterpretation as stratigraphy. Undesired return of signal (clutter) or anomalous reflection due to the surface roughness and porosity can result in ambiguity in the interpretation of data. Similarly, dielectric variation cannot be directly associated with subsurface stratification of interest such as the one associated with ice [153]. Hence, radar data are most meaningful when supported by geochemical and spectral measurements, so when combined with NIR, neutron and gamma spectrometry and in situ analyses determine elemental composition and thermophysical properties. This multi-sensor synergy reduces ambiguity and strengthens resource prospecting models by linking radar dielectric signatures to material composition and stratigraphy observed across scales.

3.7. Permittivity Sensing

Permittivity sensing (PS) is a geophysical technique used to characterize the electrical properties of planetary regolith, providing indirect information on subsurface structure, composition, porosity, and the presence of volatiles. On the Moon, dielectric permittivity is primarily controlled by regolith density, grain size, temperature, mineralogy, and the abundance of ice or other hydrogen-bearing phases. Measurements are typically obtained using radar instruments or in situ sensors that infer permittivity through the interaction of electromagnetic waves with the subsurface, including signal reflection, attenuation, and phase delay.

In addition to orbital radar observations (Section 3.6), in situ dielectric and permittivity sensors deployed on landers or rovers provide high-resolution measurements of the near-surface regolith. These instruments typically operate through direct contact or shallow penetration, measuring permittivity, conductivity, and loss tangent over the upper decimeters of the subsurface. Such measurements enable local-scale characterization of regolith density, porosity, layering, and mechanical properties, offering direct constraints for excavation, drilling, and material handling relevant to ISRU operations [154]. In polar environments, in situ permittivity measurements can help discriminate between dry regolith and ice-bearing mixtures when interpreted in conjunction with temperature and neutron data, although they remain sensitive to environmental conditions and require careful calibration. Consequently, in situ dielectric sensors provide essential ground truth for validating orbital permittivity estimates and reducing uncertainties in site-scale resource assessments [155].

3.8. Microwave Radiometry

Microwave radiometers (MWRs) are passive remote sensing instruments that detect the natural electromagnetic radiation emitted by a planetary body in the microwave spectrum (typically from 1 GHz to 200 GHz). Microwave emission at brightness temperature from a solid body surface is a measure of the physical temperature of the subsurface, weighted by the dielectric properties (which depend on density, mineralogy, and composition) of the subsurface material; the measure can also inform on the presence of subsurface heterogeneity including boulders and voids. Unlike active radars that send a signal and measure the echo, MWRs sense the spontaneous thermal emission of the subsurface, providing a unique window into the internal physical and chemical properties of the planet [156]. Compared to TIR, the key advantage is penetration depth: while the former only senses the top few microns of terrain, microwaves can penetrate the regolith from a few centimeters to several meters, depending on the operational frequency.

The primary heritage for lunar MWR comes from the first CLEP missions, Chang'e-1 and Chang'e-2, that carried the CE Lunar Microwave Sounder (CELMS) instruments into lunar orbit. They operated at four frequencies (3.0, 7.8, 19.35, and 37 GHz), acquiring the data necessary to create the first global map of the Moon's microwave brightness temperature [157]. Recent data post-processing allowed the creation of a local-time brightness temperature model to generate lunar subsurface maps that are continuous and self-consistent in both spatial and temporal domains [158]. Through an unconventional use in a new experimental radiometric mode, the DFSAR of Chandrayaan-2 studied deeper subsurface thermal emissions at L and S bands (1.25 GHz and 2.5 GHz) [159].

In terms of resource prospecting, the sensitivity of dielectric constants to mineral composition allows MWR to map metal-rich deposits such as ilmenite [160]. Furthermore, comparing data across different frequencies enables researchers to estimate regolith thickness and measure internal heat flow, which is vital for locating radioactive elements or geothermal anomalies. A particularly high-potential application involves searching for subsurface water ice in permanently shadowed regions, where microwaves can detect the unique thermal and dielectric signatures of buried volatiles that infrared sensors cannot reach. However, the technology can only guarantee a spatial resolution often restricted to tens of kilometers. Also, the significant calibration complexity makes it difficult to decouple physical temperature from material emissivity without integrating external thermal datasets.

3.9. Mass Spectrometry

Mass spectrometry (MS) is a core analytical technique for in situ chemical characterization, operating by ionizing atoms or molecules from a sample, separating the resulting ions based on their mass-to-charge ratios using electromagnetic fields, and detecting them to reconstruct the chemical composition with high specificity and sensitivity. The ion sputtering can be naturally induced by sun irradiation or by an artificial source generating a primary ion focused beam like in Secondary Ion Mass Spectrometry (SIMS). Mass analyzers such as quadrupoles are instruments commonly used in-flight for their balance of mass, power, and dynamic range, while most modern separation techniques such as ion traps or time-of-flight systems provide enhanced sensitivity and resolution for complex mixtures [161]. This capability makes mass spectrometry uniquely suited to detect trace volatiles and isotopes under vacuum conditions such as in planetary science, where this technique enables direct identification of volatiles, major elements, minor species, and isotopic ratios with minimal sample preparation [162], critical in scientific fields including exosphere characterization and astrobiology.

Historically, the Lunar Atmospheric Composition Experiment (LACE) mass spectrometer deployed during the NASA Apollo 17 mission in 1972 remains the only instrument to operate on the lunar surface for in situ volatile analysis [163]; its measurements, while sparse, provided constraints on the tenuous lunar exosphere's species and temporal variability. On board the NASA orbiter Lunar Atmosphere and Dust Environment Explorer (LADEE), the Neutral Mass Spectrometer (NMS) was also used to measure the mass distribution of neutral species in the thin lunar atmosphere over a mass-to-charge (m/z) range between 2 and 150 [164]. Beyond the Moon, mass spectrometry has already been successfully adopted on Mars by the Sample Analysis at Mars (SAM) suite, installed on NASA's MSL rover. SAM includes a quadrupole mass spectrometer coupled with a gas chromatograph and tunable laser spectrometer; it has analyzed Mars' atmosphere and volatiles released from subsurface samples, detecting organic molecules and tracing isotopic ratios [165]. As a laboratory technique, the Inductively Coupled Plasma Mass Spectrometry (ICP-MS) makes use of an ion source to vaporize, atomize and ionize the sample before using a quadrupole to detect most periodic table elements, even if present at trace

level. Because of the complexity and size of the instruments, it was successfully used on returned samples from Apollo and recently Chang'e missions for rapid and highly sensitive analytical detection [166].

In support of lunar prospecting, mass spectrometers could allow identification, quantification, and characterization of volatile resources such as water, adsorbed OH, CO_2 and other species present in the lunar regolith. By heating in ovens or using laser desorption, volatiles can be released and delivered to a mass analyzer to determine chemical composition down to trace level with high specificity and sensitivity, essential data to evaluate resource abundance and the chemical forms of the resources. Moreover, the ability to measure isotopic ratios can potentially support interpretations of resource origins, transport and deposit processes, and as such informing on water provenance. The coupling with ovens, pyrolysis, and chromatographic separation enables the analysis of both gas phase and complex solid matrices, critical for a comprehensive resource assessment [167].

Despite its powerful analytical capabilities, this technique requires complex hardware, as regolith heating or laser desorption systems impose stringent mechanical and thermal constraints. Moreover, significant mass and power demands complicate accommodation on rovers and landers. Finally, its high sensitivity poses a further challenge, since low-abundance species can be masked by ambient background signals and outgassing contamination.

3.10. Raman Spectroscopy

Raman spectroscopy (RS) is a measurement technique based on inelastic scattering of monochromatic light, typically from a laser source: when photons interact with molecular bonds or crystal lattices, a small fraction undergoes energy shifts corresponding to vibrational or rotational transitions. These shifts, measured relative to the excitation wavelength, form a Raman spectrum that acts as a molecular and mineralogical fingerprint [168]. In planetary instruments, the architecture includes a strong monochromatic exciting source and highly efficient spectral measurement apparatus, where the scattered light is collected through optical elements, filtered to suppress Rayleigh scattering, dispersed by a spectrometer and detected using CCD or Complementary Metal-Oxide-Semiconductor (CMOS) arrays. Because Raman signals are inherently weak (approximately 10^{-6}–10^{-8} of incident photons), instrument design prioritizes optical throughput, detector sensitivity, and background rejection [169].

The measurement principle and the instrument configuration make the technique suitable for in situ applications, especially on landers and rovers. The Raman spectral features are sharp and allow elimination of the ambiguity of detection that can derive from spectroscopical observations, where overlapping of features can occur in the case of compounds [170]. Hence, the principal application is the ground truth of hydrous and anhydrous minerals and ices, in a region of interest identified by orbital observation.

To date, no Raman spectrometer has yet operated on the lunar surface, while this technique has reached operational maturity on Mars. NASA's Perseverance rover carries two Raman-capable instruments: the Scanning Habitable Environments with Raman & Luminescence for Organics and Chemicals (SHERLOC) [171], a deep-UV Raman and fluorescence spectrometer mounted on the rover's robotic arm for fine-scale mineralogy and potential organic compounds with micrometer-scale spatial resolution; SuperCam [172], which integrates Raman, Laser-Induced Breakdown Spectroscopy (LIBS) (see Section 3.11), and visible/infrared spectroscopy for remote mineralogical analysis at standoff distances up to several meters. In 2030, The Raman Laser Spectrometer (RLS) is expected to operate as payload of the ESA's ExoMars Rosalind Franklin rover, analyzing powdered subsurface samples delivered from depths up to 2 m. The heritage in Mars missions and

laboratory simulations of lunar regolith analogues provide strong technical confidence in its applicability to lunar surface measurements.

For resource prospecting, Raman spectroscopy offers several compelling advantages. Firstly, it enables the direct identification of hydrated minerals and hydroxyl-bearing phases, and thus the discrimination between structurally bound OH in silicates and molecular water ice. This distinction is critical when evaluating resource extraction strategies, because it leads to different processes and levels of energy. Second, Raman spectroscopy can identify volatile-bearing phases, such as carbonates or sulphates, which may represent reservoirs of oxygen or other extractable elements. The technique is highly sensitive to O–H vibrational modes, making it effective for identifying hydrated minerals and water ice. Its ability to differentiate mineral polymorphs informs both geological interpretation and processing feasibility [169]. Structural sensitivity enables differentiation between mineral phases with identical elemental composition but distinct crystal structures, critical for assessing processing requirements. The measurement provides insight into regolith maturity and space-weathering effects, which influence volatile retention and mobility. Although Raman spectroscopy is generally unable to directly identify npFe0, it effectively reveals the associated mineral structural changes, amorphization, and glassy components. Detecting these spectral modifications indirectly constrains the presence of nanophase iron and helps predict mineral processing behavior. In PSRs, where water ice is expected to exist in mixed regolith matrices, Raman spectroscopy could verify the presence of crystalline versus amorphous ice and detect associated salts.

Raman spectrometers directly probe mineral structures without requiring sample ionization or vacuum pumping systems, reducing mechanical complexity in comparison to mass spectrometers. It is non-destructive and requires minimal sample preparation, and thus can precede more invasive techniques. The associated hardware can be miniaturized with moderate power demands and can operate under vacuum, wide thermal excursions, and radiation exposure [173]. At the same time, low scattering efficiency and signal-to-noise ratio under certain environmental conditions demand robust thermal control to maintain the laser and detector stabile under exposure to extreme temperatures of long-term operation in lunar polar regions.

While excellent for phase identification, Raman spectroscopy is less straightforward for absolute abundance quantification, compared to mass spectrometry or neutron spectroscopy. Furthermore, they can probe only the top few micrometers of a sample, with limitations in subsurface volatiles detection. For these reasons, as well as for other techniques, Raman is adopted as part of scientific packages and in conjunction with other instruments. Raman characterizes solid-phase mineral hosts, while mass spectrometry quantifies released volatiles during heating: the synergy between these techniques provides a comprehensive understanding of both abundance and chemical form. Raman spectrometers are also often coupled with LIBS (see Section 3.11) or fluorescence imaging, providing structural and compositional information, including identification of mineral polymorphs, hydrated phases, and certain organic compounds.

3.11. Laser-Induced Breakdown Spectroscopy

Laser-Induced Breakdown Spectroscopy (LIBS) is an elemental analysis technique based on the generation of a laser-induced plasma on a target surface. A high-energy pulsed laser (typically nanosecond pulses in the 1064 nm or 532 nm range) is focused onto a small spot, producing rapid heating, material ablation and plasma formation. As the plasma cools, excited atoms and ions emit light at characteristic wavelengths. The emitted spectrum, dispersed through a spectrometer and recorded by detectors, provides direct information on the elemental composition of the targeted materials [174]. The architecture of the instrument includes a pulsed laser, a focusing optics, a telescope for plasma light

collection, spectrometers covering UV–visible–near-infrared ranges and time-gated detectors to discriminate plasma continuum emission from discrete line emissions. As reported in [175], LIBS is particularly attractive for planetary surface missions because it provides a rapid and multi-element detection, with no need of sample preparation and the possibility to operate in vacuum or low-pressure environments. The measurement enables standoff analysis of rocks at meter-scale distances; for instance, ChemCam aboard NASA's Curiosity rover performed elemental analysis at distances up to 7 m, enabling rapid geochemical surveys without rover repositioning. Using the same collection optics, the Remote Micro Imager (RMI) provides context images of the LIBS analysis spots [176]. ChemCam has provided quantitative measurements of major rock-forming elements (Si, Fe, Mg, Ca, Na, K, Ti) and trace elements (e.g., Li, Sr), significantly improving geochemical mapping and stratigraphic interpretation of Gale crater on Mars. The next-generation SuperCam instrument aboard NASA's Perseverance rover integrates LIBS with Raman and infrared spectroscopy and includes microphone measurements to characterize plasma acoustics under Martian conditions; it shows improved detector sensitivity, spectral range and calibration approaches [177]. During the mission Tianwen-1 started in 2021, the Chinese Martian rover Zhurong operated in the Utopia Planitia region the scientific suite Mars Surface Composition Detector (MarSCoDe); as part of it, the LIBS instrument was recently supported by a library of spectral dataset that enhances the capability of MarSCoDe to interpret hydrous minerals [178].

To date, the only laser-induced plasma spectroscopy science instrument operated on the Moon was the Low-energy Eyesafe Laser-Induced Breakdown Scope (LE-LIBS), part of the payload of the ISRO Chandrayaan-3 mission. Landed at a southern higher latitude in August 2023, the Pragyaan rover used the LE-LIBS to detect presence of elements, notably, O, Al, Si, Ca, Fe, Ti, manganese (Mn) and chromium (Cr), in 25 different locations in the proximity of the landing site [179]. Recent results in [180] about the efficiency of LE-LIBS to detect hydrogen, helium and oxygen, have demonstrated the expected applicability of this type of instrument in an airless body such as the Moon. Ongoing instrument development programs are advancing compact LIBS packages tailored to lunar vacuum conditions, recognizing its suitability for rapid compositional surveys. In fact, since the plasma formation mechanism depends on ambient pressure, LIBS is expected to behave differently between the Martian thin atmosphere and the near-vacuum conditions of the Moon; in fact, the plasma confinement reduction under vacuum is expected to affect line intensities and calibration strategies during future lunar operations [175].

LIBS's successful operation on Mars demonstrated robustness and scientific value in rapid elemental analysis, allowing simultaneous detection of most rock-forming elements and accelerating compositional mapping. For lunar resource prospecting, LIBS offers strong capability in identifying oxide resources, metal concentrations, and geological heterogeneity at high spatial resolution. LIBS can potentially be suitable for identifying elements relevant to lunar resource utilization, including O (via oxide-forming elements such as Si, Fe, Mg, Al, Ti), H in hydrated phases, structural materials such as Fe and Al, as well as REEs [181]. Hydrogen detection by LIBS, although more complex due to weak emission lines and potential spectral interference, could help identify hydrated minerals or hydrogen-bearing regolith components, especially when integrated with complementary techniques such as NS and Raman. Additionally, LIBS enables high spatial sampling density, allowing hundreds of points to be analyzed per day without sample handling; this is advantageous for prospecting missions that must evaluate landing sites quickly to assess economic viability. Limitations of this technique are the high demand of peak power for the laser operation and the capability to ablate only the first tens of micrometers of the target material. A preliminary calibration is made quite complex due to the different behavior of the plasma expansion in local environmental conditions.

3.12. Indirect Information

On board orbital and surface platforms, other families of sensors embarked with scientific and technological purposes can also indirectly reveal the presence, abundance and position/accessibility of certain resources:

- *Light Detection and Ranging (LIDAR)* payloads hosted on planetary orbiters allow high-resolution terrain mapping and DEMs, as well as reflectance measurement (albedo) at laser wavelengths. The calculation of bolometric temperatures and illumination maps can be correlated to the conditions of potential water ice presence [182].
- *Seismometers* deployed on the surface allow the measurement of propagation velocity in the regolith. Key parameters in the process are porosity, mechanical properties and composition, but data handling and interpretation are complicated by the low wave conductivity of regolith. The phenomenon is also significantly affected by the presence of small amounts of ice in the terrain [183,184]. Numerical simulations using a 2D digital twin of the Moon's shallow subsurface structure are used to confirm the effectiveness of this technique [185]. The project "Seismic Interferometry for Moon in-situ resources exploration" (ESA Grant I-2024-01380) was initiated by ESA in 2024 with the aim to developer seismic interferometry methods for the determination of the lunar soil structure and composition.
- *Magnetometers* are adopted to measure magnetic fields, while they can also identify "Lunar Swirls" and crustal anomalies. These anomalies can shield the surface from solar wind weathering, potentially affecting the hydration cycles of the regolith and indicating the presence of metallic-rich impact melt sheets [186].
- *Engineering tools* including *drilling systems* and *penetrometers*, by means of torque control systems and monitoring of real-time drilling telemetry, enable indirect assessment of the physical and mechanical properties of the lunar soil. The mechanical resistance encountered during excavation is a proxy for regolith density and, in some regions, for the presence and concentration of volatiles in cryogenic conditions such as subsurface ice [187].

3.13. Comparative Analysis of the Measurement Techniques

In light of the considerations discussed so far, no single technology is sufficient on its own or universally optimal for comprehensive lunar resource identification; each category offers a different level of effiectiveness, tailored to specific prospecting measurement conditions and targets such as volatiles, minerals or elemental composition. A typical example is the varying effectiveness with respect to the atomic number (or weight) of the species: while XRS instruments are highly effective for mapping heavier rock-forming elements, they lack the sensitivity required for low-atomic-number element detection. In contrast, NSs excel in identifying light nuclei, particularly hydrogen, as the similar mass of neutrons and protons allows for highly efficient energy transfer and moderation.

The following comparative Table 1 further elucidates the instruments' respective effectiveness in lunar prospecting, providing an assessment of their capability to identify and, where feasible, quantify the presence of elements and materials of interest, both from orbit and in situ. Moreover, based on their technological maturity and flight heritage, their most relevant strengths and weaknesses are highlighted. The comparison does not include downstream operational aspects beyond prospecting, such as the feasibility of accessing, excavating, extracting, and transporting resources, which are strongly governed by factors such as local topography. Landing on the surface enables the extraction of subsurface samples for direct analysis through high-fidelity techniques such as LIBS and Raman, which can determine the crystalline structure and elemental purity of the ice.

Table 1. Critical comparison of main instruments employed in lunar resource prospecting.

	Resource Identification and Quantification Potential	Strengths	Limitations
Instruments *Primary use*			
Remote Sensing			
Visible camera (PAN/Multispectral) *Context characterization*	Identify—low: Morphology and albedo can reveal terrain features and structures, possibly related to its mineralogical composition Quantify—very low: species abundance extremely hard to assess	Critical for context characterization and implications (i.e., illumination and volatiles stability). In situ activities preparation.	Very poor information about terrain composition. No possibility to investigate subsurface. Dependent on illumination conditions.
Spectrometer (VNIR/SWIR) *Accurate mineralogy mapping*	Identify—high: spectral features, mineral phases (pyroxene, olivine, plagioclase, glass), hydration (OH/H_2O) Quantify—medium: efficient surface abundance, risk of ambiguity (requires modeling)	Essential for global mineral and hydration features mapping. Sensitive to trace surface amounts (although with limited resolution).	No quantification of elements abundance. Limited to first μm. Signal weakened in shadow by space weathering and mixing. Quantitative mass% uncertain.
Thermal infrared spectrometer *Specific resources distribution*	Identify—high: mineralogical (glass vs. crystalline silicate composition) and thermophysical properties as indirect indicators Quantify—low: semi-quantitative mineral fractions and thermal inertia	Critical for mapping crustal heterogeneity, silicates distribution and thermal properties.	Limited resolution. Highly sensitive to diurnal temperature variation. Coarse compositional discrimination in complex mixtures.
Gamma-ray spectrometer *Elemental composition mapping*	Identify—very high: undoubted detection of high-atomic-number elements with strong gamma emission Quantify—high: providing absolute element abundance and concentrations in weight percent	Essential for global mapping of specific (heavy) elements. Penetrates tens of cm into the subsurface.	Poor spatial resolution from common orbits. Lower or neglectable sensitivity to low-atomic-number elements and trace REE, unless concentrated.
X-Ray spectrometer *Precise elements mapping*	Identify—high: detection of major elements (Al, Mg, Si, Fe, Ti) Quantify—high: accurate elemental wt% for sampled spot and elemental ratios	Geochemical characterization. Major element mapping. Direct measurement, unaffected by mineralogy.	Poor spatial resolution from common orbits. Effective only during high solar activity (mitigated by using of active sources). Low penetration (μm).
Neutron spectrometer *Regional-scale volatile prospecting*	Identify—high (but selective for hydrogen): presence of H (proxy for H_2O/ice or H in minerals) Quantify—high: epithermal-neutron suppression unambiguous for H mass(model-dependent)	Highly efficient, also at depth of mm to meter. Independence from lighting conditions.	Spatial resolution is typically km scale. Cannot distinguish chemical form of H (ice vs. hydroxyl vs. bound H).
Radar (SAR or GPR) *Subsurface morphology and composition*	Identify—medium: detection of massive ice and subsurface structures Quantify—low: uncertain volume estimation based on CPR	Unique capability of penetration (beyond first meters). Information on resource distribution.	Resolution is poorer, compared to other instruments. High computation effort is needed. Ambiguity in data interpretation.

In Situ Measurement			
Permittivity sensor *Local characterization of regolith*	Identify—medium: bulk ice fraction and porosity via dielectric constant and thermal conductivity measurements Quantify—medium: combined with radar/GPR can constrain ice volume fraction and layer thickness	Requires contact sensors and/or well-characterized calibration samples.	Interpretation depends on matrix composition and temperature.
Mass spectrometer *In situ chemical characterization*	Identify—high: detection of volatiles, gases, molecular species, isotopes with high specificity and sensitivity Quantify—high: abundances and isotopic ratios, also allow for interpretation of resources' possible origin	In situ mass spectrometers can quantify many species. On returned samples, it provides the highest precision for trace elements and REE.	Need for sample preparation. Complexity of the necessary hardware—high mass and power demand. Obscuration of trace elements by background.
Raman spectrometer Direct probing of minerals' structure	Identify—medium: mineral phases, hydroxyl/structural H in minerals, oxidation state (indirect) Quantify—low: primarily identification and relative phase proportions; quantification of mineralogy possible with calibration	Excellent hydrated minerals and phase identification. Minimal preparation, easy and robust operation in situ.	Requires contact/near-contact instruments. Limited to solid phase. Low penetration (μm) Sensitivity to crystalline phases.
Laser-induced breakdown spectrometer Fast and distributed elemental composition	Identify—medium: elemental composition from meters; hydrogen detection Quantify—low: semi-quantitative with calibration and standards (especially for major/minor elements)	Good for rapid surveys and heterogeneity mapping, at high spatial resolution. High spatial sampling density	High demand of power. Ablation of few μm. Requires calibration and models to reach high quantitative accuracy.

An integrated approach based on the combination of different techniques is key to a comprehensive and unambiguous assessment. The search for water ice is a case in point: via remote sensing, structural mapping of regions of interest such as PSRs must then be combined with NS for hydrogen detection and quantification; thermal models enabled by TIR and illumination maps could also confirm the presence of environmental conditions for volatile stability.

In Figures 2 and 3, the effectiveness of various categories of remote sensing and in situ instruments for lunar resource prospecting is assessed and ranked on a scale 0-4, for orbital and surface measurements, respectively. Performance ratings are mapped across distinct *Prospecting functions* (namely Context Identification/Speculation, Mineralogy Definition, Elemental Quantification, Subsurface Access) against a selected subset of *Resources*. Specifically, the analysis focuses on key lunar materials, namely, Th, Ti, Fe, and volatiles (water, hydrogen, and hydroxyl). Other major rock-forming elements of interest for ISRU, such as Si, Al, Mg, and Ca, were intentionally omitted from this specific matrix to preserve chart readability. The rating intensity levels were qualitatively assigned by the authors, reflecting the performance of current state-of-the-art instrument designs and synthesized from the comprehensive literature review presented in this paper. These ratings reflect the established scientific consensus regarding the preferential performance of specific instrument classes for detecting different elements, molecules, and minerals. The Mineralogy Definition metric is intended to assess the capability to resolve specific mineral phases and crystalline structures, which is decoupled from Elemental Quantification,

herein defined as the measurement of absolute elemental or molecular abundances (e.g., wt% or ppm). Mineralogy Definition can also be inferred and supported through the identification of specific proxy elements; for this reason, for example, the effectiveness ratings assigned to instruments such as GRS and LIBS fall in the medium-to-high range.

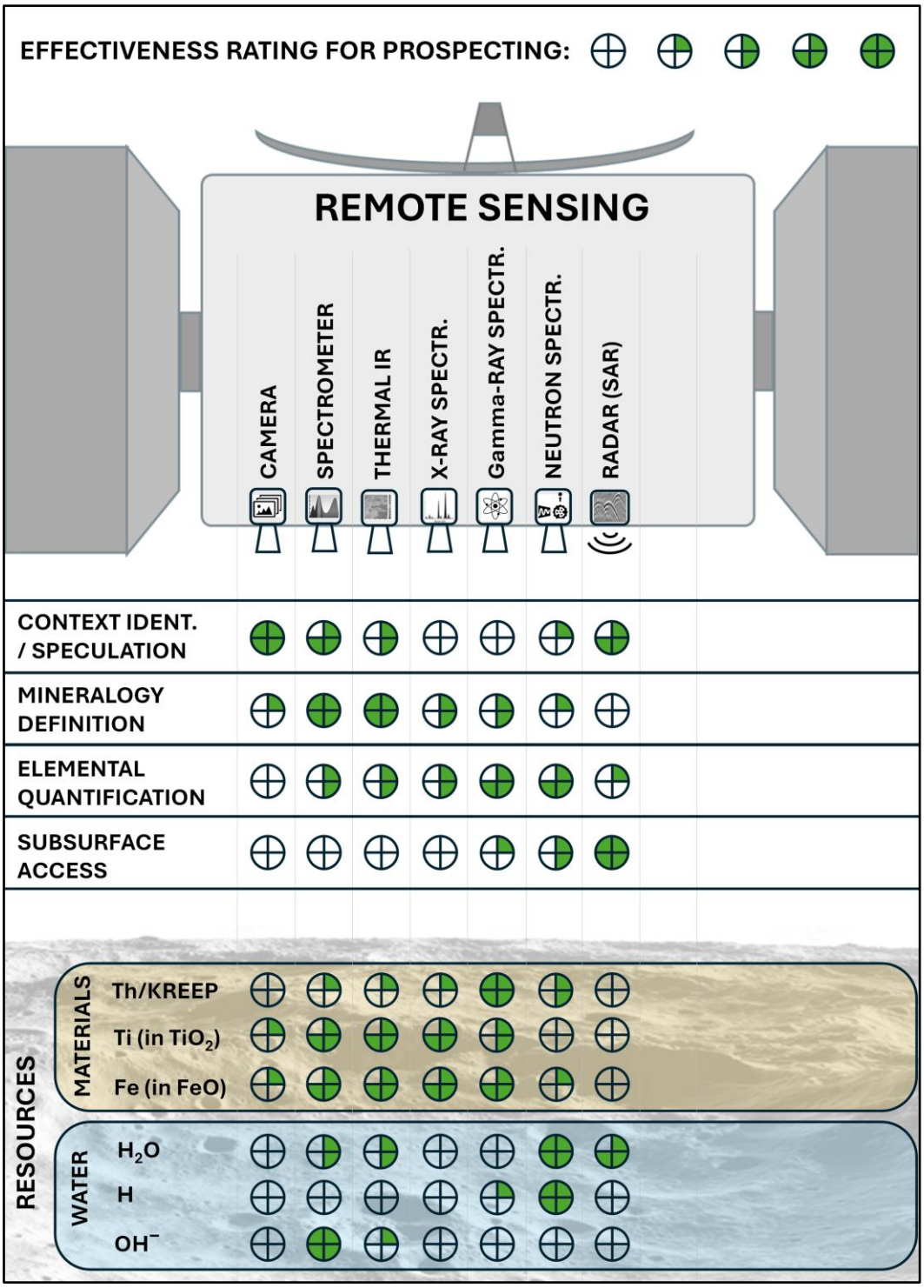

Figure 2. Estimated effectiveness matrix of remote sensing instruments for lunar resource prospecting. The effectiveness rating (on a 0–4 scale, represented by the quarter-filled circles, ranging from ineffective – empty to highly effective - full) is intended as a simplified, notional assessment. It does not account for technological maturity (i.e., instruments with different flight heritage are compared). Mineralogy Definition can be inferred and supported through the identification of specific proxy elements (e.g., Th as a proxy for KREEP is only indicative of enriched terrains).

https://doi.org/10.3390/rs18234063

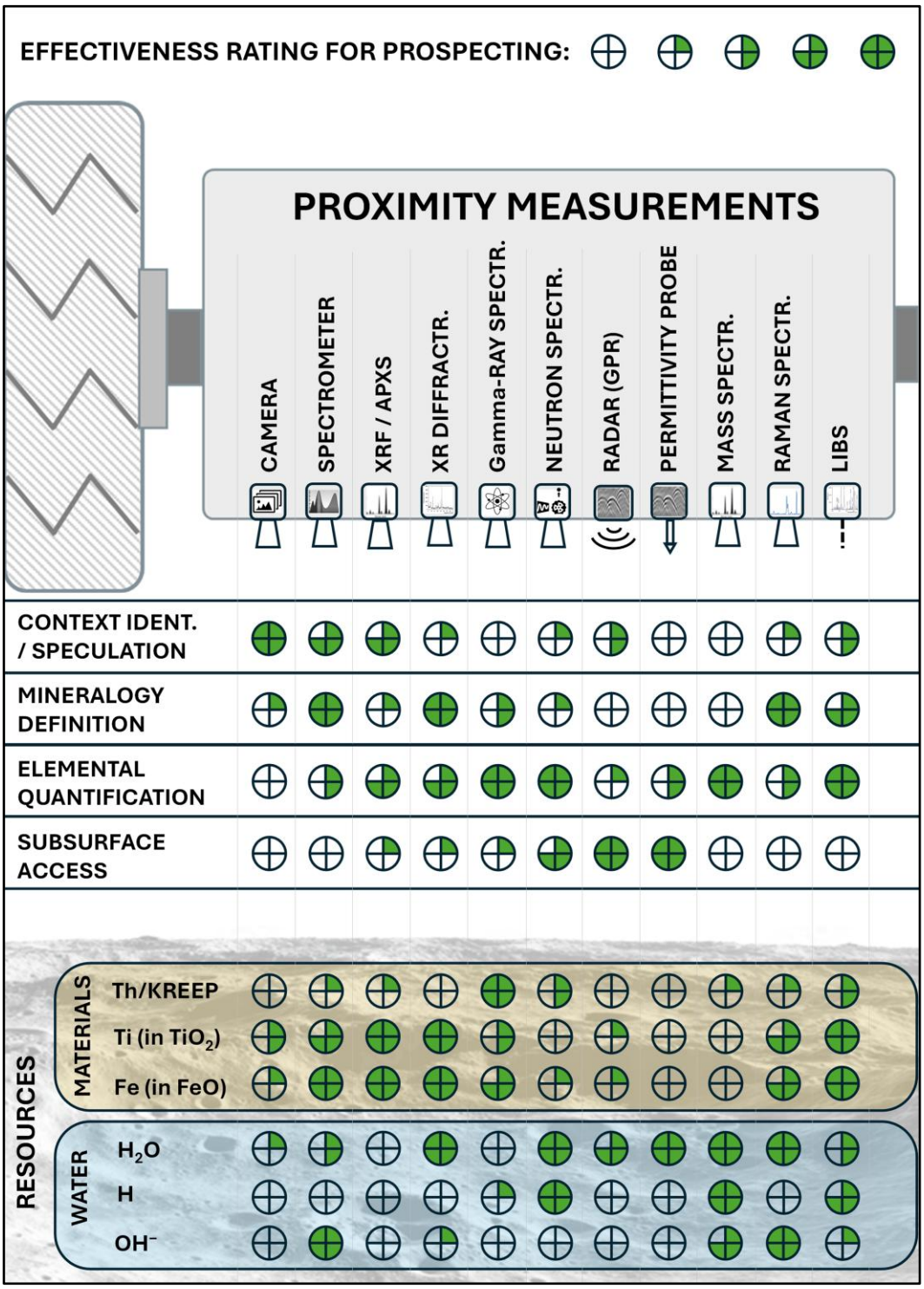

Figure 3. Estimated effectiveness matrix of in situ instruments for lunar resource prospecting. The effectiveness rating (on a 0–4 scale, represented by the quarter-filled circles ranging from ineffective – empty to highly effective - full) is intended as a simplified, notional assessment. It does not account for technological maturity (i.e., instruments with different flight heritage are compared). Mineralogy Definition can be inferred and supported through the identification of specific proxy elements (e.g., Th as a proxy for KREEP is only indicative of enriched terrains).

The transition from orbital to in situ prospecting shifts the analytical focus from regional mapping to high-fidelity local characterization of chemistry and mineralogy. While remote sensing instruments suffer from signal dilution, surface payloads provide direct, in situ validation of tightly constrained sampling areas. Although remote sensing cameras

and spectrometers can be adapted for surface operations by modifying their observational geometry, other instruments based on alternative measurement principles, such as mass and Raman spectrometers, are intrinsically designed for proximity and contact operations only.

Rather than providing an absolute, high-precision metric of individual instrument performance, this assessment aims to qualitatively identify the instrument families best-suited for specific tasks and to evaluate how they can be synergistically coupled, leveraging their complementarity, to achieve comprehensive prospecting of key resources.

4. Towards a New Phase of Resource Prospecting

The scientific probes of the last few decades generated datasets with a value for resource prospecting that was often incidental to their original mission objectives. A relevant example is reported in [46] where volatile signatures from eight instruments across 65 PSRs were combined to estimate the position and size of water ice deposits, informing landing site selection for ISRU and sustained exploration. This study also showed how large the candidate regions for resources are, highlighting the need for coordinated, rather than isolated, exploration campaigns.

Considering the relevance of ISRU in the present global space scenario, the sole speculative or inferred presence of resources is not adequate to support modern exploration programs. A more rigorous process should be established and adopted as a first, enabling step. In [188], a universal framework as common base has been introduced and proposed, with the aim to enable integration, identification of knowledge gaps and the comparison of different processing routes, in turn guiding the research strategy.

A complete and structured approach was recently proposed by the USGS, translating and adapting its long-term heritage in terrestrial resource assessment [15]. Resource detection is expected to be complemented by the information on resource quantity, status, nature and origin, thereby clarifying the feasibility of accessing, extracting, and ultimately utilizing these resources in a viable manner. A resource can then be considered a *reserve*, defined as "*a portion of the technically recoverable resource that can be converted to a commodity within budgetary and other mission constraints*". The proposed quantitative assessment methodology goes beyond mere resource prospecting, since it comprises several interrelated tasks: the identification of resources of potential interest, their quantification in terms of volume and distribution, the characterization of their physical and chemical properties, and the evaluation of their accessibility under realistic and predefined mission constraints. A focus on the first step of quantitative assessment, namely the use of descriptive models derived from Earth's mineral resources heritage, is reported in [189], where the spatial distribution of ilmenite deposits is predicted by connecting it to this Ti-bearing mineral's nature, composition and formation process. Spatial distribution is closely linked to the accessibility of the resource, a key parameter for targeting productive ISRU. To support such spatial mapping, a recent analysis introduces a standardized classification system for lunar regolith based on soil maturity and agglutinate content, offering a structured taxonomy for mapping physical and compositional properties relevant to ISRU [190].

This systematic approach can support resource utilization strategies based on scientifically validated knowledge rather than assumptions, reducing uncertainty in mission planning, and informing future investment decisions. Similarly to other disciplines of the space sector, ISRU is nowadays attracting interest from private actors, supported by technological developments and national space policies. However, the development of a sustainable lunar resource economy will depend on the availability of reliable information on the existence, quantity, distribution and accessibility of resources. As reported in [191], the sole identification of the most promising areas where the presence of resources was inferred may be not sufficient to support investment decisions. The authors therefore

highlight the potential role of space agencies in supporting systematic prospecting campaigns and generating the information required to evaluate future resource utilization scenarios.

The economic feasibility of lunar resource utilization remains uncertain and depends on several technical and operational assumptions. In [192], a Net Present Value (NPV) analysis of a lunar ice mining project suggested that public–private partnerships could offer a more favorable economic scenario than a strictly private model, especially when publicly funded exploration provides shared geological information and reduces investment risks. Similar considerations regarding the role of public–private cooperation in future space activities are discussed in [193], where the paradigms of the New Space Economy and the actual and future role of the private sector are analyzed in the context of space scientific missions. A very recent financial framework analysis reported in [194] confirmed that resolving upstream geological uncertainty via systematic prospecting is a critical prerequisite for de-risking lunar mining ventures. Concurrently, lifecycle cost analyses in [195] show that early surface habitation elements (such as Moon Base modules) can act as a high-value anchor market for locally produced oxygen and water, outperforming propulsion-focused scenarios in avoided Earth-resupply penalties.

Lunar ISRU is going to become a complex, multi-layered field where different disciplines and actors need to operate together. Similarly to mining or oil and gas sectors on Earth [27], it requires the seamless integration of diverse expertise, such as Geosciences and Prospecting for identifying volatiles and mineral concentrations, Chemical Engineering to develop closed-loop processing plants, Robotics and Civil Engineering for autonomous excavation and 3D-printing of habitats, and Legal and Economic Frameworks to define resource rights and commercial viability.

To support the multidisciplinary nature of lunar resource exploration and utilization, dedicated entities have been established, such as the European Space Resources Innovation Centre (ESRIC) in Luxembourg. Founded through a collaboration between the Luxembourg Space Agency (LSA) and the Luxembourg Institute of Science and Technology (LIST), in strategic partnership with ESA, ESRICaims to bridge scientific research and industrial applications through technological research and development, support for commercial startups, and the development of an interdisciplinary space resources ecosystem. Notably, the Lunar Resource Reference Model under development at the ESRIC establishes a standardized, traceable workflow that links heterogeneous remote sensing datasets to geological interpretations and resource indicators, proving essential for making uncertainty propagation explicit and supporting early-stage exploration decision-making.

4.1. The Transition from Planetary Science

A synergistic relationship exists between scientific exploration and resource prospecting. Science-driven missions prioritize measurements and investigations aimed at answering broad questions raised by the research community. Complementarily, the search for resources to enable ISRU imposes stricter operational requirements to achieve an accurate quantitative assessment. This synergy operates at multiple levels: for instance, determining the geological context directly informs the large-scale characterization of mineral deposits. At the same time, the high-density datasets generated during ISRU prospecting campaigns will provide unprecedented in situ, local insights into regolith properties and broader lunar processes. Understanding this mutual interdependence is essential when examining how heritage instrumentation, methodologies, and analytical models developed for traditional planetary science can be effectively transferred and adapted to meet operational ISRU needs.

The technologies, models and methods consolidated over the past few years to generate data for scientific investigations should now be converted to support the specific task of resource prospecting. Several adaptations may be envisaged:

- The basic measurement principles and instrument architectures could be maintained as reference to guide the design. Nevertheless, instrument performance requirements must respond to different needs. For instance, higher sensitivity and signal-to-noise ratios can improve detection limits, enabling the identification of lower abundances of materials and elements.
- The development process of the instruments, from design to manufacturing, testing and calibration, can follow a traditional flow. Dedicated reference standards and calibration protocols will be necessary to ensure the consistency and comparability of measurements collected by different teams, laboratories, and instrument generations. In the case of in situ measurements, the exposure to harsher environmental conditions for potentially longer periods will require increased robustness and tolerance to hazards including radiation and dust.
- Optimized measurement strategies should combine high-sensitivity measurements with distributed mapping at local scales, providing adequate spatial density and, where possible, depth coverage to characterize deposit heterogeneity. Beyond detection, abundance and composition must be assessed to inform accessibility and extractability.
- Data inversion, data analysis and data fusion methods, although based on the strong heritage consolidated in decades of space science, will require substantial customization for resource prospecting applications. Data formats and processing workflows should facilitate the integration of measurements from different instruments and their analysis using conventional and advances computational methods, including machine learning.

As for scientific investigations, the goal of a comprehensive and robust resource prospecting can be achieved only by the combination of complementary data generated by instruments different in nature and performances. Nevertheless, the integration and post-processing of measurements are strongly affected by the different characteristics of the data sources involved. Accurate crosscalibration between instruments is essential for integrating measurements acquired using different equipment, calibration procedures, and observational conditions. Indeed, although outside the scope of this review, sample-return analyses remain a critical external calibration reference against which the remote sensing and in situ measurements discussed here are validated.

To mitigate these limits, new concepts of space instruments merging multiple capabilities in one single hardware are under design. The HYPerspectral Stereo Observing System (HYPSOS) is a novel remote sensing push-broom instrument under prototyping, capable of simultaneously acquiring both three-dimensional and spectral information of the observed features. It will combine a digital terrain model obtained via a stereo camera and the compositional information generated by an embedded spectrometer, to obtain a full 4-dimensional hypercube dataset [196]. Among the most complete packages targeting resources, the ESA Package for Resource Observation and in-situ Prospecting for Exploration, Commercial exploitation and Transportation (PROSPECT) was designed to study the distribution of volatiles and to map the presence of water ice in the lunar soil. This suite can extract subsurface regolith from depths of up to one meter using the PROSPECT Sample Excavation and Extraction Device (ProSEED) robotic drill and deliver it to the PROSPECT Sample Processing and Analysis (ProSPA) analytical laboratory, a manifold of sealed ovens where it undergoes thermochemical processing and evolved gas analysis at temperatures reaching up to 1000 °C [197]. ProSPA also includes an ion trap and a magnetic sector mass spectrometer, the first instruments of this kind to be operated on the

lunar surface, for detailed elemental and isotopic measurements. The ProSEED drill is designed not only as a sampling tool of the lunar subsurface but is also equipped with sensors for monitoring permittivity and temperature, as well as drilling telemetry. Temperature variations during drilling may provide information on the physical properties of the sampled material and help monitor conditions that could affect volatile preservation. The overall goal of PROSPECT is to quantify the abundance and isotopic composition of volatiles, such as water ice and solar wind-implanted elements, while also testing the feasibility of resource extraction.

Near-real-time availability of measurements and, ideally, interpreted prospecting results will be critical during the surface operations: in particular, in the case of crewed missions, the time available for the various tasks will be a critical operational constraint. Algorithms based on machine learning that are already adopted for massive data processing (see for example [198]) could be integrated into compact instrument suites to support data processing and interpretation on the field. The expertise gained by the ESA in astronaut training allowed the elaboration of concepts for such devices, such as the Novel Portable Handheld Combined Spectrometers for Lunar Surface Exploration (PHOENIX) described in [199].

4.2. Upcoming Resources-Oriented Projects and Missions

In line with this trend, resource prospecting has recently entered the list of main priorities of the current season of exploration: while the exploitation of the scientific datasets is still in progress, a new generation of missions and payloads are under development with the declared aim of searching and quantifying those elements that can be categorized as resources, which are thus suitable for ISRU purposes.

Recent sample-return missions have also contributed to the characterization of potential lunar resources. Chang'e-5 and Chang'e-6 returned samples from the lunar near side and far side, respectively, enabling laboratory analyses relevant to the identification and characterization of lunar materials. Since 2020, Chang'e-5 confirmed the presence of water-bearing glass beads [200–202]. Using the combined data of LMS in situ and of the Nano Secondary Ion Mass Spectrometry (NanoSIMS) on Earth, the process of water formation was associated with multiple sources [203]. Investigations related to KREEP and helium-3 are also relevant to the broader characterization of lunar resources [151]. Having landed in 2024 in the vicinity of the SPA basin on the far side of the Moon, Chang'e-6 provided access to deep-crustal materials and rare elements identification, again benefitting of samples returned to the Earth [204]. Building on these investigations, Chang'e-7 will target the lunar south polar region, with instruments designed to investigate water and other potential resources. Planned to land in 2027 near the Moon Shackleton crater, its measurements are expected to advance scientific knowledge as well as to enable resource prospecting, in particular of water, in the polar regions. Specifically, the mission will operate an extremely complete set of instruments, combining orbital remote sensing (among others, including NS, GRS, and hyperspectral spectrometers) with in situ surface and subsurface investigations conducted by a lander and rover, including GPR and Raman spectrometer [205]. A key innovation is the mini flying probe (hopper), which is designed to leap directly into PSRs, to perform in situ sampling and analyze water molecules and hydrogen isotopes.

Orbital observations continue to improve the spatial characterization and quantification of lunar resources. KPLO carries the Korean Gamma-Ray Spectrometer (KGRS), which measures gamma rays over a broad energy range to investigate the elemental composition of the lunar surface. Its performance is comparable to the previous orbital gamma-ray spectrometers despite its reduced mass. Initial results include elemental maps of radioactive elements, such as K, Th, and U [206], while subsequent studies have

improved their quantitative interpretation through spatial response modeling and detector efficiency simulations [207]. The extended mission until 2027 will allow longer integration times, potentially reduce statistical uncertainties and improve the detection of localized elemental variations [208].

Commercial lunar delivery services are also expanding opportunities for deploying scientific and resource-oriented instruments. Through NASA's CLPS program, missions such as Firefly Aerospace's Blue Ghost Mission 1, have demonstrated the deployment and operation of multiple scientific payloads on the lunar surface. Among them, the Stereo Cameras for Lunar Plume-Surface Studies (SCALPSS) collected calibrated stereo imagery to characterize plume-surface interactions [209], while the Lunar Instrumentation for Subsurface Thermal Exploration with Rapidity (LISTER) measured subsurface temperatures and thermal conductivity to depths of approximately 1 m, providing information relevant to regolith physical properties [210]. The Puli Lunar Water Snooper (PLWS), a miniature neutron spectrometer intended to investigate hydrogen-bearing materials, was also included in the IM-2 missions, although its operations were limited by the non-nominal landing [211].

A major objective of upcoming resource-oriented missions is to complement orbital observations with local, in situ measurements capable of characterizing resource abundance, distribution and subsurface variability. Orbital datasets provide essential regional information but are limited by their spatial resolution, sensing depth and uncertainties in the interpretation of measured signals. Mobile surface platforms equipped with complementary instruments can help address these limitations, providing measurements at the scales required for detailed resource assessments.

The Lunar Polar Exploration (LUPEX) mission is a strategic partnership between JAXA, providing the launch vehicle and rover, and ISRO, providing the lander. Its primary objective is the in situ quantitative and qualitative assessment of lunar volatiles and water ice in the lunar south polar region. The rover combines a drill capable of sampling to depths of approximately 1.4 m with the Resource Investigation Water Analyzer (REIWA), which includes the Lunar Thermogravimetric Analyzer (LTGA), Tripe-reflection reflectron (TRITON), Aquatic Detector using Optical Resonance (ADORE), and a Raman spectrometer. Complementary instruments, including the Advanced Lunar Imaging Spectrometer (ALIS), ground-penetrating radar, neutron spectroscopy and mass spectrometry, will provide additional information on the composition and distribution of subsurface materials [212].

The Rashid Rover 3, under development by the Mohammed Bin Rashid Space Centre (MBRSC), is also expected to investigate the geological and compositional characteristics of the lunar south polar region [213]; its payload includes Moon Infrared Spectrometer (MoonIS), a VIS-IR spectrometer derived from the heritage of the ESA ExoMars Mars Multispectral Imager for Subsurface Studies (MaMISS) [214]. MoonIS will acquire hyperspectral measurements to investigate H_2O/OH signatures, mineral composition and their spatial distribution, contributing to the characterization of potential resources and local geological conditions.

Designed as a cornerstone of the Artemis program, NASA Volatiles Investigating Polar Exploration Rover (VIPER) is specifically designed to investigate the distribution and characteristics of lunar volatiles in the south polar region, including permanently shadowed regions [215]. The VIPER rover, currently planned for delivery to the lunar surface in 2027 on Blue Origin's MK1 lander, combines the Regolith and Ice Drill for Exploring New Terrain (TRIDENT), capable of sampling to approximately 1 m, with the Mass Spectrometer Observing Lunar Operations (MSOLO), enabling the investigation of volatile composition and its variation with depth. This combination was also adopted in the Polar Resources Ice Mining Experiment (PRIME-1), on board the IM-2 lander [216]. Additional

instruments include the Near-Infrared Volatiles Spectrometer System (NIRVSS), for characterizing sampled materials, and the Neutron Spectrometer System (NSS), for detecting hydrogen-bearing materials. Together, these measurements aim to improve understanding of volatile abundance, spatial distribution and subsurface variability, providing information relevant to future resource assessments [130].

Other programs, including NASA's Payloads and Research Investigations on the Surface of the Moon (PRISM), support the development and deployment of scientific instruments addressing strategic knowledge gaps relevant to lunar exploration. These include investigations of regolith properties, surface composition and environmental conditions. Lunar Vertex, selected for delivery through CLPS, will investigate the local magnetic anomaly associated surface features of Reiner Gamma [217]. The Nova-C lander will also deploy several other NASA and commercial payloads, such as the Korean LUSEM and ESA's Moon Laser Instrumentation for General relativity High accuracy Tests (MoonLIGHT) Pointing Actuator (MPAc) [218]. An overview of planned CLPS payloads is provided in [219], while continuous consulting of the CLPS program webpage is recommended for more efficient updates.

Moreover, in the paradigm of the New Space Economy, the role of the private sector is not limited to the upstream segment (i.e., the design, preparation, and implementation of missions). A novel interplay between institutional space agencies and private stakeholders is emerging within the downstream sector, creating a reciprocal marketplace for raw and processed datasets. Historically, planetary remote sensing and in situ data products were managed exclusively by governmental institutions and the scientific community under open-access frameworks, such as NASA's Planetary Data System (PDS). The data streams that will soon be available through private companies will introduce unprecedented cross-procurement dynamics. Space agencies will increasingly rely on buying commercial data products to fill critical knowledge gaps in an effective and timely fashion, without relying solely on dedicated public missions. ESA is a pioneer in this approach; as one of its first initiatives, the "Request for Information: Commercial Lunar Data Products for Exploration Science" was released in July 2026 by the Human and Robotic Exploration Directorate, to consider options for commercially procuring lunar data products that could contribute to achieving ESA's exploration science objectives. Conversely, private stakeholders will ingest historical institutional data into advanced platforms, such as digital twin environments, to de-risk their surface operations. This transactional data sharing on a commercial basis will be vital also for a rigorous resource assessment, allowing the required fusion of large amounts of data and, ultimately, the formalization of resource reserves. The evolution from science-driven, speculative exploration to a data-driven commodity market will catalyze a robust, multi-stakeholder ISRU ecosystem, paving the way for the establishment of the desired sustained and sustainable human presence on the Moon and beyond.

Such initiatives could complement existing datasets and contribute to more comprehensive resource prospecting and assessment, provided that the data quality, provenance, uncertainty and interoperability are adequately addressed. Despite the advances in lunar resource prospecting enabled by past and ongoing missions, several critical knowledge gaps remain.

First, the abundance, chemical form and physical state of lunar volatiles remain insufficiently characterized, requiring direct sampling and analysis complemented by neutron and infrared spectroscopy, as planned for missions such as VIPER and LUPEX.

Second, the subsurface distribution and heterogeneity of potential resources are still poorly constrained, highlighting the need for depth-resolved measurements through drilling, ground-penetrating radar and dielectric sensing, as envisaged for LUPEX, VIPER and Chang'e-7.

Third, the quantitative characterization of elemental and mineralogical abundances at local scales remains limited, requiring complementary in situ spectroscopic and geochemical measurements to validate and refine orbital observations. Missions such as Chang'e-7 and Rashid Rover 3 are expected to contribute to this objective. Finally, the physical and geotechnical properties governing resource accessibility and extractability remain insufficiently characterized, requiring direct measurements of regolith properties and drilling behavior, as partially addressed by instruments aboard LUPEX and VIPER.

Across all these areas, improved calibration, integration of multi-scale datasets and explicit characterization of measurement uncertainties will be essential for translating resource detections into reliable quantitative assessments. Although upcoming missions will contribute to reducing these knowledge gaps, their limited spatial coverage and predominant focus on polar volatiles highlight the continued need for coordinated prospecting campaigns, including dedicated investigations of mineral resources.

5. Conclusions

ISRU stands as the fundamental cornerstone for ensuring a viable, long-term lunar exploration; to this aim, a reliable resource evaluation necessitates a rigorous process that starts from high-fidelity prospecting based on multiple datasets from remote sensing and in situ measurements. This review and systematic analysis confirmed that existing scientific instrumentation and related data processing, when subjected to targeted customizations, possess significant potential to support ISRU. This highlights a bidirectional relationship between science and ISRU: while science-driven missions prioritize broad geological discovery, resource prospecting requires higher quantitative accuracy, sub-meter spatial resolution, and depth profiling datasets; these are the same ones that will, in turn, enrich planetary science itself.

The primary goal of this work was not mere bibliographic recording, but the examination of the performance of science-driven instruments in resource prospecting, to inform the preparation of future exploration campaigns. While scientific missions remain the real foundation of our present knowledge of lunar resources, their inherent limitations in enabling comprehensive resource prospecting were identified and discussed.

The main knowledge gaps identified in this review include the reliance on indirect measurements and compositional proxies, limited spatial and subsurface coverage, insufficient quantitative characterization of resource abundance and physical properties, and the need for improved integration and validation of complementary datasets. As discussed in Section 4.2, upcoming missions are expected to partially address these gaps through direct volatile analysis, depth-resolved investigations, in situ compositional measurements and regolith characterization. Nevertheless, coordinated multi-scale prospecting campaigns, integrated instrument suites and explicit uncertainty characterization remain essential to advance towards reliable quantitative resource assessments. In fact, the comparative analysis of measurement techniques conducted in this study reinforces the necessity and effectiveness of aggregating complementary instruments into multi-sensor, integrated payload suites, which overcome challenges and limitations due to a posteriori data analysis and crosscalibration. Future payload configurations should pair elemental sensors (e.g., LIBS, APXS, NS/GRS) with mineralogical/volatile analyzers (e.g., Raman, IR, and MS) and subsurface geophysical tools (e.g., GPR) on mobile platforms capable of operating in extreme environments. Such a synergistic architecture is already being adopted in the upcoming prospecting missions CNSA's Chang'e-7, JAXA/ISRO's LUPEX and NASA's VIPER.

The success of this preparatory work, ranging from payload and mission design to advanced data fusion, depends on a close coordination between institutional and private stakeholders. Furthermore, it cannot overlook the active involvement of the scientific

community as the custodian of key heritage in measurements, data processing, and modeling. In the next decades, a global and coordinated effort is expected, under the guidance of governments and agencies; their critical role will range from a long-term funding of prospecting campaigns to the stimulation of a robust market as an anchor customer. Only through such a collaborative cross-sector framework can we establish the virtuous and sustainable ISRU cycle required for the next season of space exploration, whose benefits will return to the Earth.

Author Contributions: Conceptualization, S.P.; writing—original draft preparation, S.P. and F.L.; writing—review and editing, S.P., F.L., A.C.D., G.C. and C.R.N.; supervision, C.R.N. and J.D.C. All authors have read and agreed to the published version of the manuscript.

Funding: This research received no external funding.

Data Availability Statement: No new data were created or analyzed in this study. Data sharing is not applicable to this article.

Conflicts of Interest: The authors declare no conflicts of interest.

Abbreviations

The following abbreviations are used in this manuscript:

ADORE	Aquatic Detector using Optical Resonance
ALIS	Advanced Lunar Imaging Spectrometer
APXS	Alpha Scattering Experiment
ASAN	Advanced Small Analyzer for Neutrals
CCD	Charge-Coupled Device
CE	Chang'e
CELMS	CE Lunar Microwave Sounder
CLEP	Chinese Lunar Exploration Program
CLPS	Commercial Lunar Payload Services
CMOS	Complementary Metal-Oxide-Semiconductor
CPR	Circular Polarization Ratio
DFSAR	Dual-Frequency SAR
DLRE	Diviner Lunar Radiometer Experiment
DTM	Digital Elevation Model
ECLSS	Environmental Control and Life Support System
ESRIC	European Space Resources Innovation Centre
ESA	European Space Agency
GPR	Ground-Penetrating Radar
GER	Global Exploration Roadmap
GRS	Gamma-Ray Spectrometry
HYPSOS	HYPerspectral Stereo Observing System
ICP-MS	Inductively Coupled Plasma Mass Spectrometry
IIRS	Imaging Infrared Spectrometer
ISECG	International Space Exploration Coordination Group
ISRO	Indian Space Research Organisation
ISRU	In Situ Resource Utilization
JAXA	Japan Aerospace Exploration Agency
KGRS	Korean Gamma-Ray Spectrometer
KPLO	Korea Pathfinder Lunar Orbiter
KREEP	Potassium (K), Rare Earth Elements (REEs), and Phosphorus (P)
LACE	Lunar Atmospheric Composition Experiment
LADEE	Lunar Atmosphere and Dust Environment Explorer
LCROSS	Lunar CRater Observation and Sensing Satellite
LELIBS	Low-energy Eyesafe Laser-Induced Breakdown Scope
LEND	Lunar Exploration Neutron Detector

LEO	Low Earth Orbit
LIDAR	Light Detection and Ranging
LIST	Luxembourg Institute of Science and Technology
LISTER	Lunar Instrumentation for Subsurface Thermal Exploration with Rapidity
LMO	Lunar Magma Ocean
LMS	Lunar Mineralogical Spectrometer
LND	Lander Neutrons and Dosimetry
LOLA	Lunar Orbiter Laser Altimeter
LORS	Lunar Ore Reserves Standards
LPR	Lunar Penetrating Radar
LRO	Lunar Reconnaissance Orbiter
LRPR	Lunar Regolith Penetrating Radar
LROC	Lunar Reconnaissance Orbiter Camera
LSA	Luxembourg Space Agency
LTES	Lunar Thermal Emission Spectrometer
LTGA	Lunar Thermogravimetric Analyzer
LTM	Lunar Thermal Mapper
LUPEX	Lunar Polar Exploration
LUSEM	Lunar Space Environment Monitor
M3	Moon Mineralogy Mapper
MaMISS	Mars Multispectral Imager for Subsurface Studies
MarSCoDe	Mars Surface Composition Detector
MBRSC	Mohammed Bin Rashid Space Centre
MoonLIGHT	Moon Laser Instrumentation for General relativity High accuracy Tests
MPAc	MoonLIGHT Pointing Actuator
MS	Mass Spectrometry
MSL	Mars Science Laboratory
MSOLO	Mass Spectrometer Observing Lunar Operations
MWR	Microwave Radiometers
NAC	Narrow Angle Cameras
NanoSIMS	Nano Secondary Ion Mass Spectrometry
NASA	National Aeronautics and Space Administration
NIR	Near-Infrared
NIRVS	Near-Infrared Volatiles Spectrometer System
NMS	Neutral Mass Spectrometer
NPV	Net Present Value
NS	Neutron spectrometry/Spectrometer
NSS	Neutron Spectrometer System
OMAT	Optical Maturity
PCAM	Panoramic Camera
PDS	Planetary Data System
PHOENIX	Novel Portable Handheld Combined Spectrometers for Lunar Surface Exploration
PKT	Procellarum KREEP Terrain
PLWS	Puli Lunar Water Snooper
PNG	Pulsed Neutron Generator
PRIME1	Polar Resources Ice Mining Experiment 1
PRISM	Payloads and Research Investigations on the Surface of the Moon
ProSEED	PROSPECT Sediment Extraction and Excretion Device
ProSPA	PROSPECT Sample Processing and Analysis
PROSPECT	Package for Resource Observation and in-situ Prospecting for Exploration, Commercial exploitation and Transportation
PSR	Permanently Shadowed Region
REE	Rare Earth Element
REIWA	Resource Investigation Water Analyzer
RIFMA	Roentgen Isotopic Fluorescent Method of Analysis
RLS	Raman Laser Spectrometer
RMI	Remote Micro Imager
RS	Raman Spectroscopy
SAM	Sample Analysis at Mars

SAR	Synthetic Aperture Radar
SCALPSS	Stereo Cameras for Lunar Plume-Surface Studies
SHERLOC	Scanning Habitable Environments with Raman & Luminescence for Organics and Chemicals
SIMS	Secondary Ion Mass Spectrometry
SNR	Signal-to-Noise Ratio
SPA	South Pole–Aitken Basin
SWIR	Shortwave Infrared
SSD	Solid State Drive
TC	Terrain Camera
TIR	Thermal Infrared/TI Radiometers
TITON	Triple-reflection Reflectron
TMC	Terrain Mapping Camera
TRIDENT	The Regolith and Ice Drill for Exploring New Terrain
USA	United States of America
USGS	United States Geological Survey
UV	Ultraviolet
VIPER	Volatiles Investigating Polar Exploration Rover
Vis	Visible
VNIR	Visible and Near-Infrared
VNIS	Visible and Near-Infrared Imaging Spectrometer
WAC	Wide Angle Camera
XRF	X-ray Fluorescence
XRS	X-ray Spectrometry/Spectrometers
XRD	X-ray Diffraction/Diffractometer

References

1. Lawrence, S.J.; Neal, C.R. Exploring the Moon in the 21st century. *Elem. An. Int. Mag. Mineral. Geochem. Petrol.* **2019**, *15*, 360–361.
2. National Aeronautics and Space Administration. Moon to Mars Objectives. 2022. Available online: https://www.nasa.gov/sites/default/files/atoms/files/m2m-objectives-exec-summary.pdf (accessed on 20 September 2026).
3. National Aeronautics and Space Administration. Moon Base: Igniting Progress. Moon Base User's Guide: Architecture Resources. April 2026. Available online: https://www.nasa.gov/wp-content/uploads/2026/04/moon-base-architecture-users-guide.pdf (accessed on 20 September 2026).
4. Wu, X. The International Lunar Research Station: China's New Era of Space Cooperation and Its New Role in the Space Legal Order. *Space Policy* **2023**, *65*, 101537.
5. ISECG. Global Exploration Roadmap 2024. August 2024. Available online: https://www.globalspaceexploration.org/wp-content/isecg/GER2024.pdf (accessed on 20 September 2026).
6. National Research Council. *The Scientific Context for Exploration of the Moon*; The National Academies Press: Washington, DC, USA, 2007.
7. Flahaut, J.; van der Bogert, C.H.; Crawford, I.A.; Vincent-Bonnieu, S. Scientific perspectives on lunar exploration in Europe. *npj Microgravity* **2023**, *9*, 50.
8. Silk, J.; Crawford, I.; Elvis, M.; Zarnecki, J. The next decades for astronomy from the Moon. *Nat. Astron.* **2023**, *7*, 648–650.
9. Rau, G.; Carpenter, K.G.; Boyajian, T.; Creech-Eakman, M.; Foster, J.; Karovska, M.; Leisawitz, D.; Morse, J.A.; Mozurkewich, D.; Peacock, S.; et al. Artemis-enabled Stellar Imager (AeSI): A Lunar long-baseline UV/optical imaging interferometer. *arXiv* **2024**, arXiv:2408.04699.
10. Harms, J.; Ambrosino, F.; Angelini, L.; Braito, V.; Branchesi, M.; Brocato, E.; Cappellaro, E.; Coccia, E.; Coughlin, M.; Della Ceca, R.; et al. Lunar gravitational-wave antenna. *Astrophys. J.* **2021**, *910*, 1.
11. Li, C.; Wang, C.; Wei, Y.; Lin, Y. China's present and future lunar exploration program. *Science* **2019**, *365*, 238–239.
12. Zhang, P.; Dai, W.; Niu, R.; Zhang, G.; Liu, G.; Liu, X.; Bo, Z.; Wang, Z.; Zheng, H.; Liu, C.; et al. Overview of the lunar in situ resource utilization techniques for future lunar missions. *Space Sci. Technol.* **2023**, *3*, 0037.
13. International Space Exploration Coordination Group. In-Situ Resource Utilization Gap Assessment Report. 2021. Available online: https://www.globalspaceexploration.org/wordpress/wp-content/uploads/2021/04/ISECG-ISRU-Technology-Gap-Assessment-Report-Apr-2021.pdf (accessed on 20 September 2026).

14. Ahrens, C.; Leone, G.; Joutsenvaara, J.; Kereszturi, A.; Calabrese, G.; Schmidt, G.W.; Bernal, A.; Palanco, S. Test mining sites at the moon: A review of resource extraction opportunities and challenges at de Gerlache, Shackleton, and Sverdrup-Henson Regions. *Eng. Geol.* **2026**, *365*, 108628.
15. Keszthelyi, L.P.; Coyan, J.A.; Bennett, K.A.; Ostrach, L.R.; Gaddis, L.R.; Gabriel, T.S.J.; Hagerty, J. *Assessment of Lunar Resource Exploration in 2022*; U.S. Geological Survey: Reston, VA, USA, 2023.
16. Espejel, C.D.; Casanova, S.; Saydam, S.; Lamamy, J.-A. Lunar ore reserves standards 101 (LORS-101). In *Handbook of Space Resources*; Springer: Berlin/Heidelberg, Germany, 2023; pp. 999–1022.
17. Wang, C.; Zhang, G.; Wang, Y.; Song, L. A review of Lunar environment and in-situ resource utilization for achieving long-term Lunar habitation. *Galaxies* **2025**, *13*, 103.
18. Glassmeier, K.-H. Solar system exploration via comparative planetology. *Nat. Commun.* **2020**, *11*, 4288.
19. The National Academies of Sciences, Engineering, and Medicine, Infrastructure for Planetary Science and Exploration. In *Origins, Worlds, and Life: A Decadal Strategy for Planetary Science and Astrobiology 2023–2032*; The National Academies Press: Washington, DC, USA, 2023.
20. Crawford, I.A.; Joy, K.H. Lunar exploration: Opening a window into the history and evolution of the inner Solar System. *Philos. Trans. R. Soc. A Math. Phys. Eng. Sci.* **2014**, *372*, 20130315.
21. Xu, L.; Li, L.; Liu, J.; Lin, H.; Li, Y.; Liu, Y.; Xie, L.; Zhang, J.; Qiao, F.; Han, J.; et al. Latest Scientific Results of China's Lunar and Deep Space Exploration (2022–2024). *Chin. J. Space Sci.* **2024**, *44*, 622–632.
22. Gaddis, L.R.; Joy, K.H.; Bussey, B.J.; Carpenter, J.D.; Crawford, I.A.; Elphic, R.C.; Halekas, J.S.; Lawrence, S.J.; Xiao, L. Recent exploration of the Moon: Science from lunar missions since 2006. *Rev. Mineral. Geochem.* **2023**, *89*, 1–51.
23. Crawford, I.A.; Anand, M.; Barber, S.; Cowley, A.; Crites, S.; Fa, W.; Flahaut, J.; Gaddis, L.R.; Greenhagen, B.; Haruyama, J.; et al. Lunar resources. *Rev. Mineral. Geochem.* **2023**, *89*, 829–868.
24. European Space Agency. Available online: https://www.esa.int/About_Us/ESA_Strategy_2040 (accessed on 20 September 2026).
25. European Space Agency. Exploration Science. Available online: https://explorationscience.esa.int/ (accessed on 20 September 2026).
26. Jones, C.A.; Klovstad, J.; Judd, E.; Komar, D. Cost breakeven analysis of cis-lunar ISRU for propellant. In Proceedings of the AIAA Scitech 2019 Forum, San Diego, CA, USA, 7–11 January 2019.
27. Sanders, G.B.; Larson, W.E. Progress made in lunar in situ resource utilization under NASA's exploration technology and development program. *J. Aerosp. Eng.* **2013**, *26*, 5–17.
28. Wieczorek, M.A.; Jolliff, B.L.; Khan, A.; Pritchard, M.E.; Weiss, B.P.; Williams, J.G.; Hood, L.L.; Righter, K.; Neal, C.R.; Shearer, C.K.; et al. The constitution and structure of the lunar interior. *Rev. Mineral. Geochem.* **2006**, *60*, 221–364.
29. Anand, M.; Crawford, I.A.; Balat-Pichelin, M.; Abanades, S.; Van Westrenen, W.; Peraudeau, G.; Jaumann, R.; Seboldt, W. A brief review of chemical and mineralogical resources on the Moon and likely initial in situ resource utilization (ISRU) applications. *Planet. Space Sci.* **2012**, *74*, 42–48.
30. Crawford, I.A. Lunar resources: A review. *Prog. Phys. Geogr.* **2015**, *39*, 137–167.
31. Anand, M. Lunar water: A brief review. *Earth Moon Planets* **2010**, *107*, 65–73.
32. Pieters, C.M.; Goswami, J.N.; Clark, R.N.; Annadurai, M.; Boardman, J.; Buratti, B.; Combe, J.-P.; Dyar, M.D.; Green, R.; Head, J.W.; et al. Character and spatial distribution of OH/H2O on the surface of the Moon seen by M3 on Chandrayaan-1. *Science* **2009**, *326*, 568–572.
33. Watson, K.; Murray, B.C.; Brown, H. The behavior of volatiles on the lunar surface. *J. Geophys. Res.* **1961**, *66*, 3033–3045.
34. Arnold, J.R. Ice in the lunar polar regions. *J. Geophys. Res. Solid Earth* **1979**, *84*, 5659–5668.
35. Nozette, S.; Lichtenberg, C.L.; Spudis, P.; Bonner, R.; Ort, W.; Malaret, E.; Robinson, M.; Shoemaker, E.M. The Clementine bistatic radar experiment. *Science* **1996**, *274*, 1495–1498.
36. Feldman, W.C.; Maurice, S.; Binder, A.B.; Barraclough, B.L.; Elphic, R.C.; Lawrence, D.J. Fluxes of fast and epithermal neutrons from Lunar Prospector: Evidence for water ice at the lunar poles. *Science* **1998**, *281*, 1496–1500.
37. Lawrence, D.J.; Feldman, W.C.; Elphic, R.C.; Hagerty, J.J.; Maurice, S.; McKinney, G.W.; Prettyman, T.H. Improved modeling of Lunar Prospector neutron spectrometer data: Implications for hydrogen deposits at the lunar poles. *J. Geophys. Res. Planets* **2006**, *111*, E08001.
38. Clark, R.N. Detection of adsorbed water and hydroxyl on the Moon. *Science* **2009**, *326*, 562–564.
39. Bhattacharya, S.; Saran, S.; Dagar, A.; Chauhan, P.; Chauhan, M.; Ajai, A.; Kumar, S.K. Endogenic water on the Moon associated with non-mare silicic volcanism: Implications for hydrated lunar interior. *Curr. Sci.* **2013**, *105*, 685–694.

40. Li, S.; Milliken, R.E. Water on the surface of the Moon as seen by the Moon Mineralogy Mapper: Distribution, abundance, and origins. *Sci. Adv.* **2017**, *3*, e1701471.
41. Mitrofanov, I.G.; Sanin, A.B.; Boynton, W.V.; Chin, G.; Garvin, J.B.; Golovin, D.; Evans, L.G.; Harshman, K.; Kozyrev, A.S.; Litvak, M.L.; et al. Hydrogen mapping of the lunar south pole using the LRO neutron detector experiment LEND. *Science* **2010**, *330*, 483–486.
42. Colaprete, A.; Schultz, P.; Heldmann, J.; Wooden, D.; Shirley, M.; Ennico, K.; Hermalyn, B.; Marshall, W.; Ricco, A.; Elphic, R.C.; et al. Detection of water in the LCROSS ejecta plume. *Science* **2010**, *330*, 463–468.
43. Schultz, P.H.; Hermalyn, B.; Colaprete, A.; Ennico, K.; Shirley, M.; Marshall, W.S. The LCROSS cratering experiment. *Science* **2010**, *330*, 468–472.
44. Sunshine, J.M.; Farnham, T.L.; Feaga, L.M.; Groussin, O.; Merlin, F.; Milliken, R.E.; A'Hearn, M.F. Temporal and spatial variability of lunar hydration as observed by the Deep Impact spacecraft. *Science* **2009**, *326*, 565–568.
45. Honniball, C.I.; Lucey, P.G.; Li, S.; Shenoy, S.; Orlando, T.M.; Hibbitts, C.A.; Hurley, D.M.; Farrell, W.M. Molecular water detected on the sunlit Moon by SOFIA. *Nat. Astron.* **2021**, *5*, 121–127.
46. Brown, H.M.; Boyd, A.K.; Denevi, B.W.; Henriksen, M.R.; Manheim, M.R.; Robinson, M.S.; Speyerer, E.J.; Wagner, R.V. Resource potential of lunar permanently shadowed regions. *Icarus* **2022**, *377*, 114874.
47. Cannon, K.M.; Britt, D.T. Accessibility data set for large permanent cold traps at the lunar poles. *Earth Space Sci.* **2020**, *7*, e2020EA001291.
48. Heiken, G.; Vaniman, D.; French, B.M. *Lunar Sourcebook: A User's Guide to the Moon*; Cambridge University Press: Cambridge, UK, 1991.
49. Saal, A.E.; Hauri, E.H.; Cascio, M.L.; Van Orman, J.A.; Rutherford, M.C.; Cooper, R.F. Volatile content of lunar volcanic glasses and the presence of water in the Moon's interior. *Nature* **2008**, *454*, 192–195.
50. Farrell, W.M.; Hurley, D.M.; Zimmerman, M.I. Solar wind implantation into lunar regolith: Hydrogen retention in a surface with defects. *Icarus* **2015**, *255*, 116–126.
51. Jones, B.M.; Carrillo-Sánchez, J.D.; Janches, D.; Sarantos, M.; Orlando, T.M. Water generation on the Moon from solar wind and meteoroid impacts. *Planet. Sci. J.* **2024**, *5*, 171.
52. Yeo, L.H.; Georgiou, A.; Morrissey, L.; Farrell, W.; McLain, J. Hydroxylation and hydrogen diffusion in lunar samples: Spectral measurements during proton irradiation. *J. Geophys. Res. Planets* **2025**, *130*, e2024JE008334.
53. Mo, L.; Xu, J.; Dong, Z.; Li, J.; Su, Y.; Ding, C. Water ice and the shallow regolith structure of the Shackleton Crater, the Moon: Implications for future Chang'E-7 in situ radar observation. *Space Sci. Technol.* **2025**, *5*, 0225.
54. Mandt, K.; Honniball, C.I.; Archer, D.; Ayala, R.A.; Captain, J.; Cohen, B.A.; Colaprete, A.; Deutsch, A.N.; Gawronska, A.J.; Hancock, M.; et al. Model for Determining the Origin of Lunar Volatiles Based on Their Composition: Application to NASA's VIPER and Other Landed Missions. *Planet. Sci. J.* **2026**, *7*, 20.
55. Gladstone, G.R.; Hurley, D.M.; Retherford, K.D.; Feldman, P.D.; Pryor, W.R.; Chaufray, J.-Y.; Versteeg, M.; Greathouse, T.K.; Steffl, A.J.; Throop, H.; et al. LRO-LAMP observations of the LCROSS impact plume. *Science* **2010**, *330*, 472–476.
56. Hurley, D.M.; Siegler, M.A.; Cahill, J.T.S.; Colaprete, A.; Costello, E.; Deutsch, A.N.; Elphic, R.C.; Fa, W.; Grava, C.; Hayne, P.O.; et al. Surface volatiles on the Moon. *Rev. Mineral. Geochem.* **2023**, *89*, 787–827.
57. Wang, Y.; Cao, H.; Chen, J.; Liu, C.; Lu, X.; Yin, C.; Fu, X.; Qiao, L.; Zhang, G.; Liu, C.; et al. New maps of mafic mineral abundances in global mare units on the Moon. *ISPRS J. Photogramm. Remote Sens.* **2025**, *224*, 348–360.
58. Binder, A.B. Lunar prospector: Overview. *Science* **1998**, *281*, 1475–1476.
59. Lawrence, D.J.; Feldman, W.C.; Barraclough, B.L.; Binder, A.B.; Elphic, R.C.; Maurice, S.; Miller, M.C.; Prettyman, T.H. High resolution measurements of absolute thorium abundances on the lunar surface. *Geophys. Res. Lett.* **1999**, *26*, 2681–2684.
60. Schluter, L.; Cowley, A. Review of techniques for In-Situ oxygen extraction on the moon. *Planet. Space Sci.* **2020**, *181*, 104753.
61. Dottori, A.; Troisi, I.; Lavagna, M. Demonstration of the low-temperature carbothermal process for producing oxygen from lunar regolith: Terrestrial test campaign. *Planet. Space Sci.* **2025**, *266*, 106154.
62. Lomax, B.A.; Selmeci, A.; Rutzler, A.; Schild, T.; Symes, M.D.; Bonsall, E.; Schroder, C.; Conti, M.; Lindner, R.; Carpenter, J.D. Identifying an efficient endpoint for oxygen extraction from lunar regolith simulant pellets using molten salt electrolysis. *Acta Astronaut.* **2025**, *234*, 287–295.
63. Robinot, J.; Rodat, S.; Abanades, S.; Paillet, A.; Cowley, A. Review of in-situ oxygen extraction from lunar regolith with focus on solar thermal and laser vacuum pyrolysis. *Acta Astronaut.* **2025**, *234*, 242–259.
64. Robinot, J.; Rodat, S.; Abanades, S.; Beche, E.; Paillet, A.; Cowley, A. Quantification of Oxygen Production from Solar Pyrolysis of Lunar Regolith. *Adv. Space Res.* **2026**, *77*, 7373–7386.

65. Burke, P.A.; Nord, M.E.; Hibbitts, C.A.; Berdis, J.R. Modeling electrolysis in reduced gravity: Producing oxygen from in-situ resources at the moon and beyond. *Front. Space Technol.* **2024**, *5*, 1304579.
66. Latini, F.; Pirrotta, S.; Mugnuolo, R.; Lavagna, M.; Troisi, I.; Dottori, A. Development Status of ORACLE, the ISRU Demonstrator for Oxygen Extraction on the Moon. In Proceedings of the IAF Space Exploration Symposium, Milan, Italy, 14–18 October 2024.
67. Guerrero-Gonzalez, F.J.; Zabel, P. System analysis of an ISRU production plant: Extraction of metals and oxygen from lunar regolith. *Acta Astronaut.* **2023**, *203*, 187–201.
68. Haskin, L.A.; Gillis, J.J.; Korotev, R.L.; Jolliff, B.L. The materials of the lunar Procellarum KREEP Terrane: A synthesis of data from geomorphological mapping, remote sensing, and sample analyses. *J. Geophys. Res. Planets* **2000**, *105*, 20403–20415.
69. Hagerty, J.J.; Lawrence, D.J.; Hawke, B.R.; Vaniman, D.T.; Elphic, R.C.; Feldman, W.C. Refined thorium abundances for lunar red spots: Implications for evolved, nonmare volcanism on the Moon. *J. Geophys. Res. Planets* **2006**, *111*, E06002.
70. Byron, B.D.; Elder, C.M.; Glotch, T.D.; Hayne, P.O.; Pigue, L.M.; Cahill, J.T.S. Evidence for Fine-grained Material at Lunar Red Spots: Insights from Thermal Infrared and Radar Data Sets. *Planet. Sci. J.* **2023**, *4*, 182.
71. Cronberger, K.; Neal, C.R. KREEP basalt petrogenesis: Insights from 15434, 181. *Meteorit. Planet. Sci.* **2017**, *52*, 827–841.
72. Zhang, Y.; Charlier, B.; Krein, S.B.; Grove, T.L.; Namur, O.; Holtz, F. The very late-stage crystallization of the lunar magma ocean and the composition of immiscible urKREEP. *Earth Planet. Sci. Lett.* **2024**, *646*, 118989.
73. Lawrence, D.J.; Feldman, W.C.; Barraclough, B.L.; Binder, A.B.; Elphic, R.C.; Maurice, S.; Miller, M.C.; Prettyman, T.H. Thorium abundances on the lunar surface. *J. Geophys. Res. Planets* **2000**, *105*, 20307–20331.
74. Yamashita, N.; Hasebe, N.; Reedy, R.C.; Kobayashi, S.; Karouji, Y.; Hareyama, M.; Shibamura, E.; Kobayashi, M.-N.; Okudaira, O.; D'Uston, C.; et al. Uranium on the Moon: Global distribution and U/Th ratio. *Geophys. Res. Lett.* **2010**, *37*, L10201.
75. Lomax, B.A.; Charpentier, G.; Nizet, A.; Rützler, A.; Suarez Kahan, A.; McDonald, F.; Lindner, R.; Carpenter, J.D. Sintering lunar regolith pellets: A comparison of four samples from Apollo 11, 15, and 16. *Mater. Today Adv.* **2025**, *28*, 100620.
76. Lucey, P.G.; Blewett, D.T.; Hawke, B.R. Mapping the FeO and TiO_2 content of the lunar surface with multispectral imagery. *J. Geophys. Res. Planets* **1998**, *103*, 3679–3699.
77. Chevrel, S.D.; Pinet, P.C.; Daydou, Y.; Maurice, S.; Lawrence, D.J.; Feldman, W.C.; Lucey, P.G. Integration of the Clementine UV-VIS spectral reflectance data and the Lunar Prospector gamma-ray spectrometer data: A global-scale multielement analysis of the lunar surface using iron, titanium, and thorium abundances. *J. Geophys. Res. Planets* **2002**, *107*, 15-1–15-14.
78. Sato, H.; Robinson, M.S.; Lawrence, S.J.; Denevi, B.W.; Hapke, B.; Jolliff, B.L.; Hiesinger, H. Lunar mare TiO_2 abundances estimated from UV/Vis reflectance. *Icarus* **2017**, *296*, 216–238.
79. Elphic, R.C.; Lawrence, D.J.; Feldman, W.C.; Barraclough, B.L.; Maurice, S.; Binder, A.B.; Lucey, P.G. Lunar Prospector measurements of the distribution of incompatible elements gadolinium, samarium and thorium. In Proceedings of the Lunar and Planetary Science Conference, Houston, TX, USA, 15–19 March 1999.
80. Elphic, R.C.; Lawrence, D.J.; Feldman, W.C.; Barraclough, B.L.; Maurice, S.; Binder, A.B.; Lucey, P.G. Lunar rare earth element distribution and ramifications for FeO and TiO_2: Lunar Prospector neutron spectrometer observations. *J. Geophys. Res. Planets* **2000**, *105*, 20333–20345.
81. Liu, S.; Du, K.; Tong, X.; Xie, H.; Feng, Y.; Jin, Y.; Wang, C.; Zhao, H.; Zhang, J. In-situ mapping of iron and titanium with the visible and near-infrared image spectrometer (VNIS) along the Yutu-2 rover traverse on the farside of the moon. *Icarus* **2024**, *412*, 116003.
82. Long-Fox, J.M.; Campins, H.; Britt, D.T. A review of technologies for lunar science, exploration, resources, and settlement. *Planet. Space Sci.* **2025**, *270*, 106229.
83. Lucey, P.G.; Blewett, D.T.; Taylor, G.J.; Hawke, B.R. Imaging of lunar surface maturity. *J. Geophys. Res. Planets* **2000**, *105*, 20377–20386.
84. Sharma, A.; Kumar, S.; Bhiravarasu, S.S. Synergistic use of remote sensing data and in-situ investigations to characterize the lunar surface. *Adv. Space Res.* **2024**, *73*, 2155–2174.
85. Haruyama, J.; Ohtake, M.; Matsunaga, T.; Morota, T.; Honda, C.; Yokota, Y.; Abe, M.; Ogawa, Y.; Miyamoto, H.; Iwasaki, A.; et al. Long-lived volcanism on the lunar farside revealed by SELENE Terrain Camera. *Science* **2009**, *323*, 905–908.
86. Haruyama, J.; Hioki, K.; Shirao, M.; Morota, T.; Hiesinger, H.; Van Der Bogert, C.H.; Miyamoto, H.; Iwasaki, A.; Yokota, Y.; Ohtake, M.; et al. Possible lunar lava tube skylight observed by SELENE cameras. *Geophys. Res. Lett.* **2009**, *36*, L21206.
87. Li, C.; Liu, J.; Ren, X.; Mou, L.; Zou, Y.; Zhang, H.; Lü, C.; Liu, J.; Zuo, W.; Su, Y.; et al. The global image of the Moon obtained by the Chang'E-1: Data processing and lunar cartography. *Sci. China Earth Sci.* **2010**, *53*, 1091–1102.
88. Kumar, A.S.K.; Chowdhury, A.R. Terrain mapping camera for Chandrayaan-1. *J. Earth Syst. Sci.* **2005**, *114*, 717–720.

89. Singh, D.; Srivastava, V.; Bhatt, J.; Bhattachary, S. Mineralogical Mapping of Lunar Orbits of Chandrayaan- 1 Mission using Hyper Spectral Imaging camera (HySI) and Terrain Mapping Camera (TMC) Data. *Photogramm. Eng. Remote Sens.* **2010**, *77*, 6–10.
90. Sinha, M.; Paul, S. Automated detection of craters on the lunar surface using deep learning: A review with insights from Chandrayaan-2 TMC-2 data. *Results Earth Sci.* **2025**, *3*, 100094.
91. Robinson, M.S.; Brylow, S.M.; Tschimmel, M.E.; Humm, D.; Lawrence, S.J.; Thomas, P.C.; Denevi, B.W.; Bowman-Cisneros, E.; Zerr, J.; Ravine, M.A. Lunar reconnaissance orbiter camera (LROC) instrument overview. *Space Sci. Rev.* **2010**, *150*, 81–124.
92. Bart, G.D.; Nickerson, R.D.; Lawder, M.T.; Melosh, H.J. Global survey of lunar regolith depths from LROC images. *Icarus* **2011**, *215*, 485–490.
93. Kloos, J.; Moores, J.E.; Godin, P.J.; Cloutis, E. Illumination conditions within permanently shadowed regions at the lunar poles: Implications for in-situ passive remote sensing. *Acta Astronaut.* **2021**, *178*, 432–451.
94. Barker, M.K.; Mazarico, E.; Neumann, G.A.; Zuber, M.T.; Haruyama, J.; Smith, D.E. A new lunar digital elevation model from the Lunar Orbiter Laser Altimeter and SELENE Terrain Camera. *Icarus* **2016**, *273*, 346–355.
95. Bilodeau, V.S.; Clerc, S.; Drai, R.; De Lafontaine, J. Optical navigation system for pin-point lunar landing. In Proceedings of the 19th IFAC World Congress, Cape Town, South Africa, 24–29 August 2014.
96. Xu, T.Y.; Hapke, B.; Zhang, X.P.; Wu, Y.Z.; Lu, X.P. Spectrophotometry of the lunar regolith using the Chang'E-3 Panoramic Camera (PCAM). *Astron. Astrophys.* **2022**, *665*, A15.
97. Chauhan, P.; Kaur, P.; Srivastava, N.; Bhattacharya, S.; Ajai; Kiran Kumar, A.S.; Goswami, J.N. Compositional and morphological analysis of high resolution remote sensing data over central peak of Tycho crater on the Moon: Implications for understanding lunar interior. *Curr. Sci.* **2012**, *102*, 1041–1046.
98. Carrer, L.; Pozzobon, R.; Sauro, F.; Castelletti, D.; Patterson, G.W.; Bruzzone, L. Radar evidence of an accessible cave conduit on the Moon below the Mare Tranquillitatis pit. *Nat. Astron.* **2024**, *8*, 1119–1126.
99. Bussey, D.B.J.; McGovern, J.A.; Spudis, P.D.; Neish, C.D.; Noda, H.; Ishihara, Y.; Sorensen, S.A. Illumination conditions of the south pole of the Moon derived using Kaguya topography. *Icarus* **2010**, *208*, 558–564.
100. Pieters, C.M.; Boardman, J.; Buratti, B.; Chatterjee, A.; Clark, R.; Glavich, T.; Green, R.; Head, J., III; Isaacson, P.; Malaret, E.; et al. The Moon mineralogy mapper (M^3) on Chandrayaan-1. *Curr. Sci.* **2009**, *96*, 500–505.
101. Green, R.; Pieters, C.; Mouroulis, P.; Eastwood, M.; Boardman, J.; Glavich, T.; Isaacson, P.; Annadurai, M.; Besse, S.; Barr, D.; et al. The Moon Mineralogy Mapper (M3) imaging spectrometer for lunar science: Instrument description, calibration, on-orbit measurements, science data calibration and on-orbit validation. *J. Geophys. Res. Planets* **2011**, *116*, E00G19.
102. Chowdhury, A.R.; Banerjee, A.; Joshi, S.R.; Dutta, M.; Kumar, A.; Bhattacharya, S.; Rehman, S.U.; Bhati, S.; Karelia, J.C.; Biswas, A.; et al. Imaging infrared spectrometer onboard Chandrayaan-2 orbiter. *Curr. Sci.* **2020**, *118*, 368–375.
103. Wu, Y.; Hapke, B. Spectroscopic observations of the Moon at the lunar surface. *Earth Planet. Sci. Lett.* **2018**, *484*, 145–153.
104. He, Z.-P.; Wang, B.-Y.; Lu, G.; Li, C.-L.; Yuan, L.-Y.; Xu, R.; Liu, B.; Chen, K.; Wang, J.-Y. Operating principles and detection characteristics of the Visible and Near-Infrared Imaging Spectrometer in the Chang'e-3. *Res. Astron. Astrophys.* **2014**, *14*, 1567–1577.
105. Li, C.; Wang, Z.; Xu, R.; Lv, G.; Yuan, L.; He, Z.; Wang, J. The scientific information model of Chang'e-4 visible and near-IR imaging spectrometer (VNIS) and in-flight verification. *Sensors* **2019**, *19*, 2806.
106. Xu, R.; Li, C.; Yuan, L.; Lv, G.; Xu, S.; Li, F.; Jin, J.; Wang, Z.; Pan, W.; Wang, R.; et al. Lunar mineralogical spectrometer on Chang'E-5 mission. *Space Sci. Rev.* **2022**, *218*, 41.
107. Williams, J.-P.; Paige, D.A.; Greenhagen, B.T.; Sefton-Nash, E. The global surface temperatures of the Moon as measured by the Diviner Lunar Radiometer Experiment. *Icarus* **2017**, *283*, 300–325.
108. Christensen, P.R.; Hamilton, V.E.; Anwar, S.; Mehall, G.; Spencer, J.R.; Sunshine, J.M.; Levison, H.F. Thermal infrared spectra of the Moon: Results from the Lucy Thermal Emission Spectrometer observations. *J. Geophys. Res. Planets* **2025**, *130*, e2024JE008493.
109. Ehlmann, B.L.; Klima, R.L.; Bennett, C.L.; Blaney, D.; Bowles, N.; Calcutt, S.; Dickson, J.; Donaldson, H.K.; Edwards, C.S.; Green, R.; et al. Lunar trailblazer: A pioneering smallsat for lunar water and lunar geology. In Proceedings of the 52nd Lunar and Planetary Science Conference, Virtual, 15–19 March 2021.
110. Sim, C.K.; Kim, S.S.; Jeong, M.; Choi, Y.-J.; Shkuratov, Y.G. Observational strategy for KPLO/PolCam measurements of the lunar surface from orbit. *Publ. Astron. Soc. Pac.* **2020**, *132*, 015004.

111. Zhang, H.; Yang, Y.; Yuan, Y.; Jin, W.; Lucey, P.G.; Zhu, M.-H.; Kaydash, V.G.; Shkuratov, Y.G.; Di, K.; Wan, W.; et al. In situ optical measurements of Chang'E-3 landing site in Mare Imbrium: 1. Mineral abundances inferred from spectral reflectance. *Geophys. Res. Lett.* **2015**, *42*, 6945–6950.
112. Adler, I.; Trombka, J.I. Orbital chemistry—Lunar surface analysis from the X-ray and gamma ray remote sensing experiments. *Phys. Chem. Earth* **1977**, *10*, 17–43.
113. Prettyman, T.H.; Hagerty, J.J.; Elphic, R.C.; Feldman, W.C.; Lawrence, D.J.; McKinney, G.W.; Vanimam, D.T. Elemental composition of the lunar surface: Analysis of gamma ray spectroscopy data from Lunar Prospector. *J. Geophys. Res. Planets* **2006**, *111*, E12007.
114. Li, Z.; Zhao, Y.; Tang, X.; Meng, Z. Optimized inversion of Chang'e-2 gamma-ray spectrum data into heat production rate for thermal evolution study: Imbrium basin as an example. *Geosci. Front.* **2026**, *17*, 102254.
115. Chen, J.; Ling, Z.; Li, B.; Zhang, J.; Sun, L.; Liu, J. Abundance and distribution of radioelements in lunar terranes: Results of Chang'E-1 gamma ray spectrometer data. *Adv. Space Res.* **2016**, *57*, 919–927.
116. Zhu, M.-H.; Chang, J.; Ma, T.; Ip, W.-H.; Fa, W.; Wu, J.; Cai, M.; Gong, Y.; Hu, Y.; Xu, A.; et al. Potassium map from Chang'E-2 constraints the impact of Crisium and Orientale basin on the Moon. *Sci. Rep.* **2013**, *3*, 1611.
117. Hong, I.-S.; Kim, S.; Kim, K.J. Data reduction and correction of Korea pathfinder lunar orbiter (KPLO) gamma-ray spectrometer (KGRS). *Earth Space Sci.* **2025**, *12*, e2024EA004181.
118. Wimmer-Schweingruber, R.F.; Yu, J.; Bottcher, S.I.; Zhang, S.; Burmeister, S.; Lohf, H.; Guo, J.; Xu, Z.; Schuster, B.; Seimetz, L.; et al. The lunar lander neutron and dosimetry (LND) experiment on Chang'E 4. *Space Sci. Rev.* **2020**, *216*, 104.
119. Litvak, M.L.; Golovin, D.V.; Djachkova, M.V.; Kalashnikov, D.V.; Kozyrev, A.S.; Mitrofanov, I.G.; Mokrousov, M.I.; Sanin, A.B.; Tret'yakov, V.I. Gamma and neutron spectrometers designed for installation onboard the lunar rover. *Sol. Syst. Res.* **2020**, *54*, 275–287.
120. Prettyman, T.H.; Englert, P.A.J.; Yamashita, N.; Landis, M.E. Neutron, Gamma-ray, and X-ray Spectroscopy of Planetary Bodies. In *Remote Compositional Analysis: Techniques for Understanding Spectroscopy, Mineralogy, and Geochemistry of Planetary Surfaces*; Cambridge University Press: Cambridge, UK, 2019; pp. 588–603.
121. Yamamoto, S.; Nakamura, R.; Matsunaga, T.; Ogawa, Y.; Ishihara, Y.; Morota, T.; Hirata, N.; Ohtake, M.; Hiroi, T.; Yokota, Y.; et al. Possible mantle origin of olivine around lunar impact basins detected by SELENE. *Nat. Geosci.* **2010**, *3*, 533–536.
122. Fu, X.-H.; Li, C.-L.; Zhang, G.-L.; Zou, Y.-L.; Liu, J.-J.; Ren, X.; Tan, X.; Zhang, X.-X.; Zuo, W.; Wen, W.-B.; et al. Data processing for the Active Particle-induced X-ray Spectrometer and initial scientific results from Chang'e-3 mission. *Res. Astron. Astrophys.* **2014**, *14*, 1595–1606.
123. Bish, D.L.; Blake, D.F.; Vaniman, D.T.; Chipera, S.J.; Morris, R.V.; Ming, D.W.; Treiman, A.H.; Sarrazin, P.; Morrison, S.M.; Downs, R.T.; et al. X-ray diffraction results from Mars Science Laboratory: Mineralogy of Rocknest at Gale crater. *Science* **2013**, *341*, 1238932.
124. Naito, M.; Hasebe, N.; Kusano, H.; Nagaoka, H.; Kuwako, M.; Oyama, Y.; Shibamura, E.; Amano, Y.; Ohta, T.; Kim, K.J.; et al. Future lunar mission Active X-ray Spectrometer development: Surface roughness and geometry studies. *Nucl. Instrum. Methods Phys. Res. Sect. A Accel. Spectrometers Detect. Assoc. Equip.* **2015**, *788*, 182–187.
125. Maruyama, Y.; Ogawa, K.; Okada, T.; Kato, M. Laboratory experiments of particle size effect in X-ray fluorescence and implications to remote X-ray spectrometry of lunar regolith surface. *Earth Planets Space* **2008**, *60*, 293–297.
126. Lawrence, D.J.; Elphic, R.C.; Feldman, W.C.; Funsten, H.O.; Prettyman, T.H. Performance of orbital neutron instruments for spatially resolved hydrogen measurements of airless planetary bodies. *Astrobiology* **2010**, *10*, 183–200.
127. Hardgrove, C.; Ayllon Unzueta, M.; Dibb, S.; Elphic, R.; Landis, M.; Reijonen, J.; Parsons, A. Active Neutron Spectroscopy for Lunar Exploration. *LPI Contrib.* **2025**, *3106*, 5025.
128. Lawrence, D.J.; Feldman, W.C.; Goldsten, J.O.; Maurice, S.; Peplowski, P.N.; Anderson, B.J.; Bazell, D.; McNutt, R.L., Jr.; Nittler, L.R.; Prettyman, T.H.; et al. Evidence for water ice near Mercury's north pole from MESSENGER Neutron Spectrometer measurements. *Science* **2013**, *339*, 292–296.
129. Wieser, M.; Barabash, S.; Wang, X.-D.; Grigoriev, A.; Zhang, A.; Wang, C.; Wang, W. The advanced small analyzer for neutrals (ASAN) on the Chang'E-4 rover yutu-2. *Space Sci. Rev.* **2020**, *216*, 73.
130. Peplowski, P.N.; Elphic, R.C.; Fritzler, E.L.; Wilson, J.T. Calibration of NASA's Neutron Spectrometer System (NSS) for landed measurements of hydrogen content of the lunar subsurface. *Nucl. Instrum. Methods Phys. Res. Sect. A Accel. Spectrometers Detect. Assoc. Equip.* **2023**, *1049*, 168063.
131. Mitrofanov, I.G.; Sanin, A.B.; Litvak, M.L.; Golovin, D.V.; Djachkova, M.V.; Anikin, A.A.; Lukyanov, N.V. Neutron emission of the lunar surface at the poles. *Cosm. Res.* **2024**, *62*, 623–631.

132. Litvak, M.L.; Mitrofanov, I.G.; Sanin, A.B.; Dyachkova, M.V. Subsurface Water Ice Content in the Cabeus Crater According to Measurements by the LEND Instrument onboard the NASA LRO Orbital Mission. *Sol. Syst. Res.* **2024**, *58*, 629–639.
133. Virkki, A.K.; Neish, C.D.; Rivera-Valentin, E.G.; Bhiravarasu, S.S.; Hickson, D.C.; Nolan, M.C.; Orosei, R. Planetary radar—State-of-the-art review. *Remote Sens.* **2023**, *15*, 5605.
134. Carter, L.M.; Campbell, D.B.; Campbell, B.A. Geologic studies of planetary surfaces using radar polarimetric imaging. *Proc. IEEE* **2011**, *99*, 770–782.
135. Spudis, P.; Nozette, S.; Bussey, B.; Raney, K.; Winters, H.; Lichtenberg, C.L.; Marinelli, W.; Crusan, J.C.; Gates, M.M. Mini-SAR: An imaging radar experiment for the Chandrayaan-1 mission to the Moon. *Curr. Sci.* **2009**, *96*, 533–539.
136. Spudis, P.D.; Bussey, D.B.J.; Baloga, S.M.; Butler, B.J.; Carl, D.; Carter, L.M.; Chakraborty, M.; Elphic, R.C.; Gillis-Davis, J.J.; Goswami, J.N.; et al. Initial results for the north pole of the Moon from Mini-SAR, Chandrayaan-1 mission. *Geophys. Res. Lett.* **2010**, *37*, L06204.
137. Bhiravarasu, S.S.; Chakraborty, T.; Putrevu, D.; Pandey, D.K.; Das, A.K.; Ramanujam, V.M.; Mehra, R.; Parasher, P.; Agrawal, K.M.; Gupta, S.; et al. Chandrayaan-2 dual-frequency synthetic aperture radar (DFSAR): Performance characterization and initial results. *Planet. Sci. J.* **2021**, *2*, 134.
138. Kochar, I.; Chakraborty, T.; Bhiravarasu, S.S.; Das, A.; Putrevu, D.; Panigrahi, R.K. Estimation of lunar surface roughness using Chandrayaan-2 full-polarimetric DFSAR data. *Icarus* **2023**, *406*, 115720.
139. Thomson, B.J.; Bussey, D.B.J.; Neish, C.D.; Cahill, J.T.S.; Heggy, E.; Kirk, R.L.; Patterson, G.W.; Raney, R.K.; Spudis, P.D.; Thompson, T.W.; et al. An upper limit for ice in Shackleton crater as revealed by LRO Mini-RF orbital radar. *Geophys. Res. Lett.* **2012**, *39*, L14201.
140. Spudis, P.D.; Bussey, D.B.J.; Baloga, S.M.; Cahill, J.T.S.; Glaze, L.S.; Patterson, G.W.; Raney, R.K.; Thompson, T.W.; Thomson, B.J.; Ustinov, E.A. Evidence for water ice on the Moon: Results for anomalous polar craters from the LRO Mini-RF imaging radar. *J. Geophys. Res. Planets* **2013**, *118*, 2016–2029.
141. Dong, Z.; Fang, G.; Ji, Y.; Gao, Y.; Wu, C.; Zhang, X. Parameters and structure of lunar regolith in Chang'E-3 landing area from lunar penetrating radar (LPR) data. *Icarus* **2017**, *282*, 40–46.
142. Ding, C.; Xiao, Z.; Su, Y.; Zhao, J.; Cui, J. Compositional variations along the route of Chang'e-3 Yutu rover revealed by the lunar penetrating radar. *Prog. Earth Planet. Sci.* **2020**, *7*, 32.
143. Dong, Z.; Fang, G.; Zhou, B.; Zhao, D.; Gao, Y.; Ji, Y. Properties of Lunar Regolith on the Moon's Farside Unveiled by Chang'E-4 Lunar Penetrating Radar. *J. Geophys. Res. Planets* **2021**, *126*, e2020JE006564.
144. Lai, J.; Xu, Y.; Bugiolacchi, R.; Meng, X.; Xiao, L.; Xie, M.; Liu, B.; Di, K.; Zhang, X.; Zhou, B.; et al. First look by the Yutu-2 rover at the deep subsurface structure at the lunar farside. *Nat. Commun.* **2020**, *11*, 3426.
145. Su, Y.; Wang, R.; Deng, X.; Zhang, Z.; Zhou, J.; Xiao, Z.; Ding, C.; Li, Y.; Dai, S.; Ren, X.; et al. Hyperfine structure of regolith unveiled by Chang'E-5 lunar regolith penetrating radar. *IEEE Trans. Geosci. Remote Sens.* **2022**, *60*, 5110414.
146. Fang, F.; Ding, C.; Feng, J.; Su, Y.; Sharma, R.; Giannakis, I. In-situ radar observation of shallow lunar regolith at the Chang'E-5 landing site: Research progress and perspectives. *Remote Sens.* **2023**, *15*, 5173.
147. Verma, N.; Bhatt, M.; Dangi, M.; Kumar, S.; Bhardwaj, A. Exploring water-ice deposits in lunar polar craters with Chandrayaan-2 DFSAR data. *Icarus* **2025**, *432*, 116492.
148. Sahu, C.; Kumar, S.; Govil, H.; Chattoraj, S.L. Integrated Analysis of Water Ice Detection in Erlanger Crater, Lunar North Pole: Insights from Chandrayaan-1 Mini-SAR and Chandrayaan-2 DFSAR Data. *Remote Sens.* **2024**, *17*, 31.
149. Shroff, U.; Shukla, S.; Patel, P.; Mohan, S. Detection of Water Ice in Faustini Crater Floor Using DFSAR. In Proceedings of the IGARSS 2024—2024 IEEE International Geoscience and Remote Sensing Symposium, Athens, Greece 7–12 July 2024.
150. Singh, A.; Sharma, A.; Kumar, S.; Chang, L.; Vashishtha, A.; Raj, R.; Agrawal, S.; Chauhan, P. Dielectric characterization and polarimetric analysis of lunar north polar crater Hermite-A using Chandrayaan-1 Mini-SAR, Lunar Reconnaissance Orbiter (LRO) Mini-RF, and Chandrayaan-2 DFSAR data. *Adv. Space Res.* **2022**, *70*, 4030–4055.
151. Ding, C.; Li, Q.; Xu, J.; Lei, Z.; Li, J.; Su, Y.; Huang, S. Moon-based ground penetrating radar derivation of the Helium-3 reservoir in the regolith at the Chang'E-3 landing site. *IEEE J. Sel. Top. Appl. Earth Obs. Remote Sens.* **2023**, *16*, 2764–2776.
152. Shen, S.; Tang, C.; Li, Y.; Lu, W.; Li, S.; Li, Z.; He, W.; Zhao, B.; Fan, G.; Liu, X.; et al. The Lunar Penetrating Radar on the Chang'E-7 Rover. *Space Sci. Rev.* **2025**, *221*, 98.
153. Lai, J.; Xu, Y.; Zhang, X.; Xiao, L.; Yan, Q.; Meng, X.; Zhou, B.; Dong, Z.; Zhao, D. Comparison of dielectric properties and structure of lunar regolith at Chang'e-3 and Chang'e-4 landing sites revealed by ground-penetrating radar. *Geophys. Res. Lett.* **2019**, *46*, 12783–12793.

154. Gscheidle, C.; Witzel, T.; Smolka, A.; Reiss, P. Permittivity sensor development for lunar and planetary surface exploration. *Front. Space Technol.* **2024**, *4*, 1303180.
155. Trautner, R.; Reiss, P.; Kargl, G. A drill-integrated miniaturized device for detecting ice in lunar regolith: The PROSPECT permittivity sensor. *Meas. Sci. Technol.* **2021**, *32*, 125117.
156. Cai, Z.; Lan, T. Lunar brightness temperature model based on the microwave radiometer data of Chang'E-2. *IEEE Trans. Geosci. Remote Sens.* **2017**, *55*, 5944–5955.
157. Chan, K.L.; Tsang, K.T.; Kong, B.; Zheng, Y.-C. Lunar regolith thermal behavior revealed by Chang'E-1 microwave brightness temperature data. *Earth Planet. Sci. Lett.* **2010**, *295*, 287–291.
158. Meng, Z.; Dong, X.; Lei, J.; Ping, J.; Cai, Z.; Zhang, X.; Huang, S.; Zhang, Y. Constructing a complete brightness temperature dataset of the moon with Chang'e-2 microwave radiometer data. *IEEE Trans. Geosci. Remote Sens.* **2023**, *61*, 5302114.
159. Renju, R.; Raju, C.S. Simulation analysis of microwave emission from lunar subsurface for SAR radiometric mode dual frequency (L/S Bands) observations onboard Chandrayaan-2. *Adv. Space Res.* **2023**, *72*, 3499–3508.
160. Siegler, M.A.; Feng, J.; Lucey, P.G.; Ghent, R.R.; Hayne, P.O.; White, M.N. Lunar titanium and frequency-dependent microwave loss tangent as constrained by the Chang'E-2 MRM and LRO Diviner lunar radiometers. *J. Geophys. Res. Planets* **2020**, *125*, e2020JE006405.
161. Ren, Z.; Guo, M.; Cheng, Y.; Wang, Y.; Sun, W.; Zhang, H.; Dong, M.; Li, G. A review of the development and application of space miniature mass spectrometers. *Vacuum* **2018**, *155*, 108–117.
162. Arevalo, R., Jr.; Ni, Z.; Danell, R.M. Mass spectrometry and planetary exploration: A brief review and future projection. *J. Mass Spectrom.* **2020**, *55*, e4454.
163. Hoffman, J.H.; Hodges, R.R., Jr.; Johnson, F.S.; Evans, D.E. 17. Lunar Atmospheric Composition Experiment. In *Apollo 17: Preliminary Science Report*; Scientific and Technical Information Office, National Aeronautics and Space Administration: Washington, DC, USA, 1973; Volume 330, p. 17-1–17-9.
164. Benna, M.; Mahaffy, P.R.; Halekas, J.S.; Elphic, R.C.; Delory, G.T. Variability of helium, neon, and argon in the lunar exosphere as observed by the LADEE NMS instrument. *Geophys. Res. Lett.* **2015**, *42*, 3723–3729.
165. Goesmann, F.; Brinckerhoff, W.B.; Raulin, F.; Goetz, W.; Danell, R.M.; Getty, S.A.; Siljestrom, S.; Missbach, H.; Steininger, H.; Arevalo, R.D., Jr.; et al. The Mars Organic Molecule Analyzer (MOMA) instrument: Characterization of organic material in martian sediments. *Astrobiology* **2017**, *17*, 655–685.
166. Zong, K.; Wang, Z.; Li, J.; He, Q.; Li, Y.; Becker, H.; Zhang, W.; Hu, Z.; He, T.; Cao, K.; et al. Bulk compositions of the Chang'E-5 lunar soil: Insights into chemical homogeneity, exotic addition, and origin of landing site basalts. *Geochim. Cosmochim. Acta* **2022**, *335*, 284–296.
167. Morse, A.D.; Abernethy, F.; Barber, S.J.; Lim, S.; Sargeant, H.; Sheridan, S.; Wright, I.P. Mass Spectrometers for In-Situ Resource Utilisation. In Proceedings of the Lunar ISRU 2019—Developing a New Space Economy Through Lunar Resources and Their Utilization, Columbia, MD, USA, 15–17 July 2019.
168. Long, D.A. *The Raman Effect: A Unified Treatment of the Theory of Raman Scattering by Molecules*; John Wiley & Sons: Chichester, UK, 2002.
169. Wang, A.; Jolliff, B.L.; Haskin, L.A. Raman spectroscopy as a method for mineral identification on lunar robotic exploration missions. *J. Geophys. Res. Planets* **1995**, *100*, 21189–21199.
170. Angel, S.M.; Gomer, N.R.; Sharma, S.K.; McKay, C. Remote Raman spectroscopy for planetary exploration: A review. *Appl. Spectrosc.* **2012**, *66*, 137–150.
171. Bhartia, R.; Beegle, L.W.; Deflores, L.; Abbey, W.; Razzell Hollis, J.; Uckert, K.; Monacelli, B.; Edgett, K.S.; Kennedy, M.R.; Sylvia, M.; et al. Perseverance's scanning habitable environments with Raman and luminescence for organics and chemicals (SHERLOC) investigation. *Space Sci. Rev.* **2021**, *217*, 58.
172. Wiens, R.C.; Maurice, S.; Robinson, S.H.; Nelson, A.E.; Cais, P.; Bernardi, P.; Newell, R.T.; Clegg, S.; Sharma, S.K.; Storms, S.; et al. The SuperCam instrument suite on the NASA Mars 2020 rover: Body unit and combined system tests. *Space Sci. Rev.* **2021**, *217*, 4.
173. Rull Perez, F.; Sylvestre, M.; Hutchinson, I.; Moral Inza, A.G.; Perez, C.; Diaz, C.; Colombo, M.; Belenguer Davilla, R.; Lopez Reyes, G.E.; Sansano Caramazana, A.; et al. The Raman Laser Spectrometer for the ExoMars Rover Mission to Mars. *Astrobiology* **2017**, *17*, 627–654.
174. Cremers, D.A.; Radziemski, L.J. *Handbook of Laser-Induced Breakdown Spectroscopy*; 2nd ed.; John Wiley & Sons: Chichester, UK, 2013.

175. Knight, A.K.; Scherbarth, N.L.; Cremers, D.A.; Ferris, M.J. Characterization of laser-induced breakdown spectroscopy (LIBS) for application to space exploration. *Appl. Spectrosc.* **2000**, *54*, 331–340.
176. Maurice, S.; Wiens, R.C.; Saccoccio, M.; Barraclough, B.; Gasnault, O.; Forni, O.; Mangold, N.; Baratoux, D.; Bender, S.; Berger, G.; et al. The ChemCam instrument suite on the Mars Science Laboratory (MSL) rover: Science objectives and mast unit description. *Space Sci. Rev.* **2012**, *170*, 95–166.
177. Maurice, S.; Wiens, R.C.; Bernardi, P.; Cais, P.; Robinson, S.; Nelson, T.; Gasnault, O.; Reess, J.-M.; Deleuze, M.; Rull, F.; et al. The SuperCam instrument suite on the Mars 2020 rover: Science objectives and mast-unit description. *Space Sci. Rev.* **2021**, *217*, 47.
178. Qu, S.-Y.; Shen, J.; Li, L.; Cui, Z.; Xu, X.; Liu, Z.; Huang, C.; Li, H.; Lin, H.; Lin, W.; et al. An Inclusive Library for Quantitative Analysis of the Laser-induced Breakdown Spectra Acquired by the Zhurong Mars Rover. *Astrophys. J.* **2025**, *994*, 260.
179. George, R.S.; Sridhar, R.V.L.N.; Supriya, G.; Prabakaran, B.; Padmasree, S.; Umesh, S.B. Development of Planetary Data Products and Future-Ready Long-Term Archival Prospects of the Chandrayaan-3 LIBS Instrument. In Proceedings of the 2025 International Conference on Computing Technologies (ICOCT), Bengaluru, India, 13–14 June 2025; pp. 1–7.
180. Sridhar, R.V.L.N.; Malathi, S.; Kumar, S.; Roy, U.M.; Sriram, K.V. Investigation of LE-LIBS feasibility for detection of H, He, and O in high vacuum using geological samples. *Opt. Lett.* **2025**, *50*, 1500–1503.
181. Wiens, R.C.; Cousin, A.; Clegg, S.M.; Gasnault, O.; Chen, Z.; Maurice, S.; Shu, R. Geochemistry of Mars with Laser-Induced Breakdown Spectroscopy (LIBS): ChemCam, SuperCam, and MarSCoDe. *Minerals* **2025**, *15*, 882.
182. Lucey, P.G.; Neumann, G.A.; Riner, M.A.; Mazarico, E.; Smith, D.E.; Zuber, M.T.; Paige, D.A.; Bussey, D.B.; Cahill, J.T.; McGovern, A.; et al. The global albedo of the Moon at 1064 nm from LOLA. *J. Geophys. Res. Planets* **2014**, *119*, 1655–1679.
183. Larose, E.; Campillo, M.; Khan, A.; Nakamura, Y. Lunar subsurface investigated from correlation of seismic noise. *Geophys. Res. Lett.* **2005**, *32*, L16201.
184. Kunimasu, T.; Sawayama, K.; Tsuji, T. Estimation of the mass fraction and distribution of ice in a lunar regolith simulant from seismic velocity. *Icarus* **2023**, *406*, 115725.
185. Keil, S.; Schimmel, M.; Igel, H. Evaluating Seismic ambient noise techniques for detecting ice-bearing rocks on the Moon. *Earth Space Sci.* **2025**, *12*, e2025EA004369.
186. Klokočník, J.; Kostelecký, J.; Cílek, V.; Bezděk, A.; Kletetschka, G. *Atlas of the Gravity and Magnetic Fields of the Moon*; Springer: Cham, Switzerland, 2022.
187. Gertsch, L.; Gustafson, R.; Gertsch, R. Effect of water ice content on excavatability of lunar regolith. *AIP Conf. Proc.* **2006**, *813*, 1093–1100.
188. Hadler, K.; Martin, D.J.P.; Carpenter, J.; Cilliers, J.J.; Morse, A.; Starr, S.; Rasera, J.N.; Seweryn, K.; Reiss, P.; Meurisse, A. A universal framework for Space Resource Utilisation (SRU). *Planet. Space Sci.* **2020**, *182*, 104811.
189. Diaz, A.C.; Keszthelyi, L. Descriptive models for lunar High-Ti deposits. *Acta Astronaut.* **2025**, *226*, 375–384.
190. Juilleret, J.; Scalenghe, R.; Diaz, A.C.; Certini, G. A classification framework for mapping lunar soils. *Soil Sci. Soc. Am. J.* **2026**, *90*, e70206.
191. Neal, C.R.; Salmeri, A.; Abbud-Madrid, A.; Carpenter, J.D.; Colaprete, A.; Hibbitts, K.A.; Kleinhenz, J.; Link, M.; Sanders, G. The Moon needs an international lunar resource prospecting campaign. *Acta Astronaut.* **2024**, *214*, 737–747.
192. Sommariva, A.; Gori, L.; Chizzolini, B.; Pianorsi, M. The economics of moon mining. *Acta Astronaut.* **2020**, *170*, 712–718.
193. Fiore, F.; Elvis, M. Space science & the space economy. *Space Policy* **2026**, *75*, 101713.
194. Smith-Vaniz, G.; Stähler, S.C.; Kehl, F. A framework for the economic evaluation of lunar mining projects. *Space Planet. Resour.* **2026**, *2*, 3.
195. Johnson, J.E.; Sowers, G.F.; Abbud-Madrid, A. The value of lunar-derived oxygen and water for an early habitation customer. *Space Planet. Resour.* **2026**, *2*, 12.
196. Cremonese, G.; Naletto, G.; Re, C.; Tordi, M.; Dorgnach, I.; Doria, C.; La, R.; Grassa, A.; Agostini, L.; Brotto, F.; et al. The HYPerspectral Stereo Observing System. *Mem. Della Soc. Astron. Ital. J. Ital. Astron. Soc.* **2024**, *95*, 66–76.
197. Trautner, R.; Barber, S.J.; Fisackerly, R.; Heather, D.; Houdou, B.; Howe, C.; Iacobellis, S.; Leese, M.; Mariani, A.; Meogrossi, G.; et al. PROSPECT: A comprehensive sample acquisition and analysis package for lunar science and exploration. *Front. Space Technol.* **2024**, *5*, 1331828.
198. Bian, C.; Zhang, K.; Wu, Y.; Wu, S.; Lu, Y.; Duan, Y.; Wu, H.; Zhao, Z.; Wu, W. New maps of lunar surface oxide abundances and Mg# using an optimized ensemble learning Algorithm. *IEEE J. Sel. Top. Appl. Earth Obs. Remote Sens.* **2025**, *18*, 9119–9134.

199. Moral, A.G.; Perez, C.; Seoane, L.; Rodriguez-Perez, P.; Parejo, M.B.; Zafra, J.; Rodriguez, J.A.; Canchal, R.; Santamaria, P.; Martin, S.; et al. PHOENIX: Novel portable handheld combined spectrometers for Lunar surface exploration. In Proceedings of the IAF Space Exploration Symposium (IAC 2024), Milan, Italy, 14–18 October 2024.
200. Lin, H.; Li, S.; Xu, R.; Liu, Y.; Wu, X.; Yang, W.; Wei, Y.; Lin, Y.; He, Z.; Hui, H.; et al. In situ detection of water on the Moon by the Chang'E-5 lander. *Sci. Adv.* **2022**, *8*, eabl9174.
201. Zhou, C.; Tang, H.; Li, X.; Zeng, X.; Mo, B.; Yu, W.; Wu, Y.; Zeng, X.; Liu, J.; Wen, Y. Chang'E-5 samples reveal high water content in lunar minerals. *Nat. Commun.* **2022**, *13*, 5336.
202. Liu, J.; Liu, B.; Ren, X.; Li, C.; Shu, R.; Guo, L.; Yu, S.; Zhou, Q.; Liu, D.; Zeng, X.; et al. Evidence of water on the lunar surface from Chang'E-5 in-situ spectra and returned samples. *Nat. Commun.* **2022**, *13*, 3119.
203. Zhou, C.; Mo, B.; Tang, H.; Gu, Y.; Li, X.; Zhu, D.; Yu, W.; Liu, J. Multiple sources of water preserved in impact glasses from Chang'e-5 lunar soil. *Sci. Adv.* **2024**, *10*, eadl2413.
204. Zhang, Q.W.L.; Yang, M.-H.; Li, Q.-L.; Liu, Y.; Yue, Z.-Y.; Zhou, Q.; Chen, L.-Y.; Ma, H.-X.; Yang, S.-H.; Tang, X.; et al. Lunar farside volcanism 2.8 billion years ago from Chang'e-6 basalts. *Nature* **2025**, *643*, 356–360.
205. Wang, C.; Jia, Y.; Xue, C.; Lin, Y.; Liu, J.; Fu, X.; Xu, L.; Huang, Y.; Zhao, Y.; Xu, Y.; et al. Scientific objectives and payload configuration of the Chang'E-7 mission. *Natl. Sci. Rev.* **2024**, *11*, nwad329.
206. Kim, K.J.; Kim, S.; Choi, Y.; Park, J.H.; Kim, Y.K.; Hong, I.-S.; Yi, E.S.; Park, K.; Lee, K.B.; Min, K.W.; et al. Overviews on major scientific results of KPLO Gamma-Ray Spectrometer (KGRS). In Proceedings of the AGU Fall Meeting, San Francisco, CA, USA, 11–15 December 2023.
207. Park, J.; Kim, K.J.; Choi, Y. Method for determining the mass concentration of natural radioactive elements on the lunar surface using the KPLO gamma-ray spectrometer. *Adv. Space Res.* **2025**, *75*, 8849–8859.
208. Jeon, M.-J.; Kim, E.; Kim, D.G. KPLO Nominal mission operation results and extended mission preparation. In Proceedings of the 45th COSPAR Scientific Assembly, Busan, Republic of Korea, 13–21 July 2024.
209. Maddock, R.; Munk, M.; Danehy, P.M.; Tyrrell, O.K.; Weisberger, J.M.; Fahringer, T.W.; Lueg, R.; Wilson, C.; Scammell, A.; Martin, K.; et al. Firefly Blue Ghost Mission 1: SCALPSS 1.1 Payload and Mission Overview. In Proceedings of the AIAA SciTech Forum, Orlando, FL, USA, 12–16 January 2026.
210. Nagihara, S.; Zacny, K.; Ngo, P.; Sanasarian, L.; Misra, R.; Zasadzien, M.; Sanigepalli, V.; Schmitt, M.; Wang, A.; Ladd, C.; et al. The Lunar Instrumentation for Subsurface Thermal Exploration with Rapidity (LISTER) on Blue Ghost Mission 1 to Mare Crisium. I. Pneumatic Excavation of Regolith. *Planet. Sci. J.* **2025**, *6*, 232.
211. Bussey, D.B.J.; Robinson, M.S.; Martin, T.D. Intuitive Machines: Enabling Commercial International Lunar Scientific Exploration. *LPI Contrib.* **2025**, *3090*, 2738.
212. Mizuno, H.; Wakabayashi, S.; Hoshino, T.; Ohtake, M.; Asoh, D. Development Status in 2024 on Lunar Polar Exploration (LUPEX) Project. Presented in IAF Space Exploration Symposium, Proceedings of the 75th International Astronautical Congress, IAC 2024, Milan, Italy, 14–18 October 2024.
213. Almarzooqi, H.; Almatroushi, H.; Els, S.G.; Almaeeni, S.; Alzaabi, M. Emirates Lunar Mission Past, Present, and Future. *LPI Contrib.* **2024**, *3063*, 5070.
214. De Sanctis, M.C.; Altieri, F.; Biondi, D.; De Angelis, S.; Rossi, L.; Ferrari, M.; Filacchione, G.; Ciarniello, M.; Formisano, M.; Frigeri, A.; et al. *MoonIS Spectrometer on RASHID Lunar Rover*; Copernicus Meetings: Finlandia Hall Helsinki, Finland, 7–12 September 2025.
215. Fernando, B.; Neal, C.; Kiraly, J.; Fernandez, B.; Patterson, R.; Gyalay, S.; Lemelin, M. The Case for Continuing VIPER: A Critical Milestone on the Journey Back to the Moon. *Planet. Sci. J.* **2025**, *6*, 289.
216. Zacny, K.; Chu, P.; Vendiola, V.; Paulsen, G.; Creekmore, P.; Goldman, S.; Bailey, J.; Ng, P.; Fortuin, C.; Stamboltsian, J.; et al. TRIDENT Ice Mining Drill for Lunar Volatile Prospecting for PRIME-1 and VIPER Missions. *Planet. Sci. J.* **2025**, *6*, 297.
217. Vines, S.; Ho, G.; Blewett, D. The Lunar Vertex PRISM Payload: Ready for the Moon. In Proceedings of the European Geosciences Union General Assembly 2024 (EGU24), Vienna, Austria, 14–19 April 2024.

218. Muccino, M.; Montanari, M.; Lauretani, R.; Remujo Castro, A.; Rubino, L.; Denni, U.; Rodriquez, R.; Salvatori, L.; Tibuzzi, M.; Filomena, L.; et al. MoonLIGHT and MPAc: The European Space Agency's Next-Generation Lunar Laser Retroreflector for NASA's CLPS/PRISM1A (CP-11) Mission. *Remote Sens.* **2025**, *17*, 813.
219. Niles, P.B. Summary of The Contracted Deliveries of NASA Payloads to the Moon via Commercial Lunar Payload Services (CLPS). In Proceedings of the Lunar and Planetary Science Conference, The Woodlands, TX, USA, 10–14 March 2025.

Disclaimer/Publisher's Note: The statements, opinions and data contained in all publications are solely those of the individual author(s) and contributor(s) and not of MDPI and/or the editor(s). MDPI and/or the editor(s) disclaim responsibility for any injury to people or property resulting from any ideas, methods, instructions or products referred to in the content.